Chapter 2

Radioactive selenium: origin and environmental dispersion scenarios

Teba Gil-Díaz, Frank Heberling and Elisabeth Eiche

2.1 INTRODUCTION

Radionuclides can be present in the environment from both natural and anthropogenic origins, showing characteristic biogeochemical behaviours according to the specific properties of the element. The environmental mobility and bioavailability of selenium (Se) strongly depends on the chemical species which, in turn, depends on aspects like redox state and microbiology. Among the most common oxidation states, species of Se(IV) and Se(VI) are considered relatively mobile and bioavailable. Once incorporated within an organism, Se shows a narrow band between dietary deficiency (e.g., used as a co-factor in functional proteins and RNA) and toxicity (e.g., selenosis, dependent on the concentrations and the chemical species involved; Jeffery *et al.*, 2002). The recommended daily intake for adult humans is limited to 1 µg kg^{-1} of body weight, with a maximum allowable concentration in drinking water of 10 µg L^{-1} (WHO [World Health Organization], 2011). In addition, Se has no essential metabolism in plants but it is still readily taken up and accumulated due to its structural similarity with other oxyanion forms of bio-essential elements like sulfate and phosphate (Pilon-Smits *et al.*, 2017).

doi: 10.2166/9781789061055_0061

Potential incorporation and accumulation due to the use of Se in the metabolism gives rise to the radiotoxicity of radioactive Se isotopes. Of all the radioactive Se isotopes, the long-lived fission product ^{79}Se shows the biggest concern with respect to the long-term dispersion from disposal sites for high-level nuclear waste and its potential radiotoxicity from beta emissions. Environmental risk assessment of radioactive Se from anthropogenic sources is still a topic of ongoing research aiming to better determine the specific dispersion paths and potential environmental impacts. This chapter will present (i) basic knowledge on radioactive Se, (ii) examples on environmental analytical techniques, (iii) current understanding of its environmental reactivity, dispersion and fate from deep geological repositories to different compartments of the geosphere, and (iv) considerations on distribution and effective doses in the biosphere.

2.2 CHARACTERISTICS OF RADIOACTIVE SELENIUM

2.2.1 Environmental persistence: half-lives and decay modes

Selenium has six stable isotopes: ^{74}Se (0.89%), ^{76}Se (9.37%), ^{77}Se (7.63%), ^{78}Se (23.77%), ^{80}Se (49.61%) and ^{82}Se (8.73%). Despite the fact that ^{82}Se is strictly an unstable nucleus, decaying into stable, gaseous krypton (^{82}Kr), it is mainly seen as a stable isotope when considering environmental processes given its extremely long half-life ($t_{1/2}$ in the order of 10^{19} y; Audi *et al.*, 2003).

From over 21 radioactive Se-isotopes, only two show half-lives long enough to render them persistent in a system ($t_{1/2}$ >1 h): ^{75}Se ($t_{1/2} = 199.78$ d; Audi *et al.*, 2003) decaying into stable ^{75}As by electron capture, and ^{79}Se ($t_{1/2} = 3.27.10^5$ y; Jörg *et al.*, 2010) decaying into stable ^{79}Br by emitting beta radiation (β^-, negatively charged high-energy electrons). From these two, only ^{75}Se releases gamma radiation (γ, photon emissions).

The production of other Se radioisotopes from parent radionuclides produced during nuclear fission (e.g., germanium, Ge) is considered to have a small contribution to the global budget of Se radioisotopes. An example would be ^{81}Se, produced via ^{81}Ge decay (^{81}Ge → ^{81}As → [^{81m}Se →] ^{81}Se → ^{81}Br; Gray *et al.*, 2007), presenting short half-lives for both ^{81}Se ($t_{1/2} = 18.45$ min) and its metastable form (^{81m}Se, $t_{1/2} = 57.28$ min). Similarly, radionuclides of ^{72}Se ($t_{1/2} = 8.40$ d) and ^{73}Se ($t_{1/2} = 7.1$ h) show relatively longer half-lives but are only produced by the radioactive decay of Br (Br → Se → As → Ge), resulting from nuclear fusion reactions in research accelerators (e.g., bombardment of ^{58}Ni with ^{16}O to produce ^{72}Br; Mihailescu & Cata-Danil, 2010). Therefore, these Se radioisotopes will not be discussed in this chapter.

2.2.2 Sources and applications

2.2.2.1 Natural geogenic ^{82}Se

The only naturally occurring radionuclide of Se (^{82}Se) originates from both volcanic emissions and the Earth's crust. The average concentrations of ^{82}Se in the Earth's crust are very low with 4–8 μg kg^{-1} (i.e., total Se content of 50–90 μg kg^{-1}; Salminen *et al.*, 2005). Its characteristic radioactive decay ($2\beta^-$) is extremely rare among radioactive emissions, also present in ^{76}Ge, ^{96}Zr, ^{100}Mo, ^{116}Cd and ^{136}Xe. Nevertheless, this radioactive decay has been extensively used in several research programmes (e.g., NEMO-3, SuperNEMO, LUCIFER/CUPID-0; Artusa *et al.*, 2017; Kaizer *et al.*, 2018) with the aim of evidencing neutrinoless double beta decay patterns, which could provide insights into the matter-antimatter asymmetry in the universe. For example, the SuperNEMO programme designs experiments improving the detection limits of double beta decay emissions for several isotopes, tracking the trajectories of the emitted electrons and determining their individual energies (Arnold *et al.*, 2010). Otherwise, specific uses of ^{82}Se include isotopically-labelled experiments in both dissolved and organic chemical forms, given its relatively low natural abundance compared to stable ^{77}Se and ^{78}Se. These studies comprise a wide range of experimental approaches, mostly in biological/ecotoxicological studies for understanding metabolic routes of Se (e.g., Ogra *et al.*, 2018; Shiobara *et al.*, 2000; Suzuki *et al.*, 2006), detoxification mechanisms of Se-bearing proteins concerning the uptake of mercury (Spiller, 2018; Yoneda & Suzuki, 1997) and isotopic fractionation during uptake (Banning *et al.*, 2013; Schilling *et al.*, 2015, 2020; Xu *et al.*, 2020).

2.2.2.2 Anthropogenic radiotracer ^{75}Se

Due to its relatively short half-life ($t_{1/2} = 199.78$ d), ^{75}Se is not naturally present nor relevant for environmental studies. In fact, it can only be produced artificially from proton bombardment of natural arsenous oxide or neutron activation from stable ^{74}Se. It may be present in the cooling pond for UO_2 fuel from light water reactors (e.g., Neeb, 1997), but it is mostly known for its paramount application related to isotopically-labelled experiments. Experimental studies widely use ^{75}Se as a radiotracer in all kinds of chemical forms, ranging from labelled organic ^{75}Se–selenomethionine to inorganic ^{75}Se–selenite, and ^{75}Se–selenate species. The reason for its extensive use in different studies is related to several points such as: (i) its ease of production and simple commercialization, (ii) its half-life, rendering it sufficiently persistent during the time period of usual laboratory experiments, (iii) its decay into stable ^{75}As in a relatively short time, facilitating the management of the radioactive waste, and (iv) its electron capture decay producing characteristic gamma lines detectable by radiometric techniques, allowing it to reach environmentally relevant concentration-levels due to the achievable detection limits in the order of

$<10^{-15}$ mol Se, equivalent to ~75 fg, and simplifying sample preparation (*c.f. Section 2.3.2*).

The use of ^{75}Se as a radiotracer serves the general interest in expanding the knowledge on the biogeochemical behaviour of Se, from both biological and environmental viewpoints. Original works initially focused on improving the understanding of sample loss during pre-treatment and the production of satisfactory figures of merit for analytical techniques quantifying Se species (e.g., hydride generation and atomic absorption spectroscopy; Campbell, 1992; Dočekal *et al.*, 1997; Krivan, 1982; Reamer *et al.*, 1981). Biological studies include a wide range of applications. For instance, many ecotoxicology studies aim at developing a fundamental understanding of Se distribution, bioaccumulation and biomagnification (e.g., in marine organisms, terrestrial plants and mammals; Araie *et al.*, 2008; Beilstein & Whanger, 1988; Einoder *et al.*, 2018; Fowler *et al.*, 1999; Reinfelder & Fisher, 1994). Other works use this knowledge on the metabolism of Se for radioactive diagnostic materials in medical science (Irons *et al.*, 2006; Yang *et al.*, 2017) and the development of new biotechnological solutions (e.g., alternatives to fertilizers for Se-deficient crops; Galinha *et al.*, 2012; Riaz *et al.*, 2018). Additionally, environmentally-oriented research works mainly focus on the sorption of Se to different solid phases in various liquid matrices in order to determine solid/liquid partitioning in pure and natural sediments for purposes of environmental risk assessment, for example, related to radionuclide mobility or plant uptake in Se-deficient areas. Some studies include scenarios of potential radionuclide dispersion from deep geological repositories (e.g., underground research laboratories such as Grimsel in Switzerland; Alexander *et al.*, 2009; Eikenberg *et al.*, 1997). The fate of Se after radionuclide accidental releases and the potential dispersion in specific environments was also studied using ^{75}Se labels (i.e., Gil-Díaz *et al.*, 2020a; Hesslein, 1987; Lee *et al.*, 2012). Other applications focus on remediation purposes concerning the decontamination of Se, among other trace elements, using environmental matrices (e.g., Santschi *et al.*, 1980; Suzuki *et al.*, 2014; Tuğrul *et al.*, 2015).

2.2.2.3 Anthropogenic ^{79}Se from nuclear fission

Many radionuclides are products of nuclear fission and may be released to the environment during nuclear power plant (NPP) accidental events (e.g., Chernobyl, Ukraine 26th April 1986, and Fukushima Dai-ichi, Japan 11th March 2011), from fuel reprocessing plants or from nuclear waste repositories. Some of these radionuclides show low fission yields (i.e., low probability of being formed during nuclear fission) but long half-lives (high persistence), and thus accumulate in the fuel and become of relevant concern over time. Out of all the potential fission products of ^{235}U and ^{239}Pu related to Se radionuclides (from ^{75}Se to ^{95}Se),

only ^{79}Se fits within these criteria and is by far the most ubiquitous radioisotope of Se in nuclear waste, contributing to the estimated total cumulative radioactive dose (ANDRA, 2005; Ikonen *et al.*, 2016). Such conditions are also the reason why ^{79}Se is scarcely registered nor followed after NPP accidental releases or from admissible daily discharges of nuclear installations (i.e., compared to other known fission products such as ^{137}Cs, ^{131}I, ^{132}Te and ^{125}Sb). In fact, ^{79}Se is rather included in the lists of radionuclides of relevance or of 'potential criticality' during decommissioning of NPPs and from potential radioactive leaks from nuclear waste disposal areas (i.e., from geological repositories; Tanaka *et al.*, 2014). In addition, ^{79}Se is also a main activation product in vitrified waste, spent fuel, hulls and endpieces surrounding the nuclear waste (NIROND, 2001). Upon potential contact of the spent fuel with groundwater, ^{79}Se is expected to be released relatively quickly. Therefore, the interest in ^{79}Se is related to its estimated, future potential environmental mobility and radiation doses from nuclear waste disposal/storage sites to the geosphere and biosphere, essential for the long-term safety assessment of geological repositories (Asai *et al.*, 2011; Hoving, 2018; Ikonen, 2017).

At a minor scale, low and intermediate level wastes are also expected to contain ^{79}Se, not only originating from the nuclear industry, but also as activation products from nuclear applications, research laboratories, and hospitals (Aguerre & Frechou, 2006). Concerning environmental evidence, only one study has reported activities of ^{79}Se in trees at the Fukushima Daiichi NPP site one year after the accident. This study classified ^{79}Se within the 'highly volatile fission products or neutron activated nuclides' together with ^{90}Sr, ^{99}Tc and ^{129}I (Tanaka *et al.*, 2014). They measured values between the detection limit of <0.05 Bq g^{-1} and maximum activities of 0.22 Bq g^{-1} (equivalent to 0.10–0.43 μg kg^{-1}). For comparison, the German radio-protection-regulations (StrlSchV, 2018) specify a maximum limit of 0.1 Bq g^{-1} of ^{79}Se for the unrestricted use of solid and liquid materials. Other studies related to risk assessment of ^{79}Se are based on ^{75}Se radiotracer behaviour in hypothetical conditions with environmentally relevant solid and liquid phases (*c.f. Section 2.2.2.2*) or on studies with stable Se-isotopes.

2.3 SAMPLE COLLECTION AND QUANTIFICATION TECHNIQUES

2.3.1 Environmental sampling

Environmental biogeochemical processes hardly distinguish between stable or radioactive isotopes. For this reason, it is generally assumed that the biogeochemical behaviour of radionuclides follows that of their analogue stable isotopes (e.g., IAEA TRS [International Atomic Energy Agency Technical Reports Series] 422). This also implies that sampling for Se radionuclides in

natural matrices follows the same procedures and precautions as for studies on stable environmental Se. A general remark can be made that for Se, no ashing procedures or strong heating should be applied as some Se species may be volatile at >70°C.

The major difference between sampling procedures for radioactive and stable isotopes would be related to the amount of sample collected. In general, sampling of radioactive elements requires larger volumes of water (e.g., >5 L, particularly in seawater) and solid masses than for the analogue stable isotopes, due to the generally low activities found in the environment. For instance, Tanaka *et al.* (2014) point out that plant material should weigh more than 30 g dry weight for radiochemical analysis of ^{79}Se. Another reason for higher sample amounts is the necessity for extensive sample pre-treatment and separation steps. In environmental samples, the radionuclide of interest often has to be pre-concentrated. Separation steps help to avoid interference with other radionuclides, enabling an accurate quantification due to, for example, the uncharacteristic beta emissions from ^{79}Se decay. In contrast, ^{75}Se can be quantified with only minor or no pre-treatment steps due to its characteristic signal from gamma radiation. Therefore, there are no established standard protocols regarding the minimum mass required for optimum quantification of Se radionuclides for specific matrices and sites. General sampling procedures and sample storage strategies for standard radiological monitoring in specific matrices are published in IAEA guidelines, for example, for water, foodstuffs, soil size fractionation and vegetation (Barnekow *et al.*, 2019; Guidebook, 1989; Joint, 2016; Martinčič, 1999).

2.3.2 Analytical methods

The main analytical methods used to quantify both ^{75}Se (gamma-emitter) and ^{79}Se (beta-emitter) are based on the respective radioactive decay signals, summarized for specific cases in Table 2.1. The most commonly applied method for ^{75}Se is gamma spectroscopy (e.g., based on a high purity Germanium HPGe or a NaI (Tl) crystal), related to its characteristic gamma energy lines (e.g., 264.7 and 136 keV energy lines). When applicable, ^{79}Se may be quantified by liquid scintillation counting (LSC) through the excitation of a mixture of reagents, sensitive to beta-radiation. Speciation of Se can be determined by using X-ray spectroscopic techniques, though few studies report measurements on radioactive Se (Table 2.1).

Noteworthy, the quantification of ^{75}Se by gamma spectroscopy is much less affected by matrix effects compared to classical spectrometric techniques (mass-MS, atomic absorption-AAS, or optical emission-OES), and can be directly applied to salt brines, seawater, or digestion solutions. These characteristics present big advantages in experimental approaches using radiotracers of ^{75}Se over spikes of Se stable isotopes. Until recently, analytical challenges in the

Table 2.1 Examples of quantification methods used in different matrices and experimental conditions concerning both ^{75}Se and ^{79}Se.

Context	Radionuclide and Matrix	Pre-treatment and/or Separation Method	Quantification Method	Reference
Spikes of ^{75}Se				
Selenoproteins in coccolithophores	Biological samples	Sonication then several purification and size fractionation steps	NaI(Tl) gamma-detector	Araie *et al.* (2008)
Se transfer from zooplankton to fish	Biological samples	Centrifugation and biochemical fractionation steps	NaI(Tl) gamma-detector (264 keV)	Reinfelder and Fisher (1994)
Se enrichment in seeds	Water and plant seeds	None specified	HPGe (136 keV)	Galinha *et al.* (2011)
Se solid fractionation in forest floors	Lake water	Soil extractions with KH_2PO_4 and NaOH; Water spikes fractionated in HPLC columns; Centrifugation	'Well-type scintillation counter'	Gustafsson and Johnsson (1994)
Se solid/liquid partitioning in estuarine sediment suspensions	River and estuarine water	Centrifugation	HPGe (264.7 keV) (DL: $<$0.03 Bq mL^{-1} in 10 mL)	Gil-Díaz *et al.* (2020a)
Se retention by mangrove sediment columns	Tidal water	None specified	HPGe	Suzuki *et al.* (2014)
Batch experiments with modified bentonites	Ultra-pure water	None specified	'High resolution gamma spectrometry'	Tuğrul *et al.* (2015)
Batch experiments with bentonite and quartz	Synthetic ground and freshwater	Centrifugation	NaI(Tl) gamma-detector (500–700 keV)	Lee *et al.* (2012)

(*Continued*)

Table 2.1 Examples of quantification methods used in different matrices and experimental conditions concerning both ^{75}Se and ^{79}Se (*Continued*).

Context	Radionuclide and Matrix	Pre-treatment and/or Separation Method	Quantification Method	Reference
Injected radioactive tracer at Grimsel Test Site	Synthetic solution	None specified	HPGe (DL: <1 Bq m^{-1} and <0.01 Bq mL^{-1} in 1 L)	Eikenberg *et al.* (1997)
Radiochemical protocol to quantify ^{79}Se	Simulated intermediate level wastes (solids)	Microwave digestion including HF	n-type Be detector (264.7 keV)	Aguerre and Frechou (2006)
Direct measurements of ^{79}Se				
Radioactive contamination after the Fukushima NPP accident	Natural tree samples (30 g)	Acid extraction with 100 mL 10M HNO_3; Elution from TEVA® Resin with HBr; Reduction by hydroxylamine; Precipitate re-dissolved in HNO_3	LSC (DL: <0.05 Bq g^{-1})	Tanaka *et al.* (2014)
Quantification in high level waste (HLW)	Spent nuclear fuel (5 g)	Digestion with 50 mL 4M HNO_3; cation exchange resin (BIO-RAD AG), eluted with 1M HNO_3	ICP-QMS	Asai *et al.* (2011)
In-vivo tracers in humans	Biological samples	None specified	AMS	Kutschera (1998)
Speciation of radioactive Se in nuclear fuel from a BWR	Spent nuclear fuel micro-particles	Preparation of sample pellets	Micro XANES	Curti *et al.* (2015)
Speciation of Se vitrified waste	Vitrified nuclear waste	Glass fragment in sample container	XAFS	Dardenne *et al.* (2015)

Abbreviations: HPGe, high purity germanium detector; DL, detection limits; HPLC, high-performance liquid chromatography; LSC, liquid scintillation counting; ICP-QMS, inductively coupled plasma quadrupole mass spectrometry; AMS, accelerator mass spectrometry; BWR, boiling water reactor; XANES, X-ray absorption near edge spectroscopy; XAFS, X-ray absorption fluorescence spectroscopy.

quantification of Se stable isotopes included important matrix effects and polyatomic/isobaric interferences of bromine hydrides (HBr), doubly-charged rare earths (REE, e.g., such as $^{164}Dy^{++}$) and/or from the argon gas (e.g., ^{82}Kr or $^{38}Ar^{40}Ar^{+}$; ^{80}Se is usually not measured due to the high abundance of $^{40}Ar^{40}Ar^{+}$). For this reason, the detection limit of all classical methods is relatively high so that it is nearly impossible to measure natural concentrations in many samples, especially when matrix dilution is required. Existing techniques to measure low levels of Se in the past included HR-ICP-MS (high resolution inductively coupled plasma mass spectrometry) or sector-field ICP-MS. But these techniques are very expensive and thus not widely distributed. Nevertheless, the current advent of new generation ICP-MS apparatus (e.g., Triple Quadrupole generation, TQ-ICP-MS) allows such interferences to be successfully overcome. This advancement provides better detection limits for quantifying trace levels of stable Se in natural samples and allows future experimental studies to use more environmentally relevant concentrations; though not yet reaching the levels achieved in radiotracer studies.

Several optical and electrochemical techniques have been suggested to show strong potential applications for on-site, field-deployable devices to monitor Se directly in freshwater and seawater (Devi *et al.*, 2017). Actual portable devices may have been developed for on-site monitoring of Se species, though with sporadic uses. An example is the portable device measuring the speciation of Se for a month in wastewaters of thermal power plants by hydride generation coupled to a chemiluminescence detector, showing relatively high detection limits (DL) of ~8 µg L^{-1} (Ezoe *et al.*, 2016). Other examples include electrochemical probes using gold nanoparticles showing DL of 0.12–0.27 µg L^{-1} for potential applications in seawater and agricultural food but no proven use in environmental monitoring (Segura *et al.*, 2015; Tan *et al.*, 2020). The use of portable XRF (X-ray fluorescence) analysis for on-site screening of Se in solid samples has been reported for nail clippings, soils, soil suspensions and animal tissues, showing DL of 0.83–1.00 mg kg^{-1} for direct analyses (Beaudette *et al.*, 2009; Fleming *et al.*, 2015). However, as the sample-instrument geometry and sample matrix strongly influence the XRF measurements, accuracy and precision, the DL can strongly vary when using portable XRF instruments. Specific pre-extraction methods applied on digested sample solutions in combination with total reflection XRF are reported to bring down the DL to 0.05 mg kg^{-1} (Marguí *et al.*, 2010). Nevertheless, such pre-treatment steps may not be easy to implement on site on a routine basis. Thus, to the best of our knowledge, there are no current on-site/field-based analytical techniques or monitoring probes being used systematically to quantify radioactive or stable Se species. Monitoring programmes until now have generally relied on classical field sample collection of environmental matrices and laboratory analyses (e.g., 30-year monitoring of the Kesterson case in San Francisco; Ohlendorf *et al.*, 2020).

2.4 PRODUCTION AND MOBILITY OF ^{79}Se IN NUCLEAR WASTE REPOSITORIES

2.4.1 Estimated activities in the nuclear waste

It is important to bear in mind that there are different types of nuclear fuel and according to its specific composition, burn-up and delay until its reprocessing or final disposal point, it may develop and present different radionuclides in variable amounts. Several simulations exist, estimating the potential radioactive levels of ^{79}Se present in spent fuel for specific conditions (i.e., nuclear reactors, fuel types, and burn-ups). For instance, a 10-y aged high-level waste from a light water reactor (LWR) may produce 3.7×10^{10} Bq y^{-1} of ^{79}Se (i.e., equivalent to ~72 g y^{-1}), which is in the same order of magnitude as estimations for ^{129}I and lower than those for ^{135}Cs, ^{137}Cs, ^{126}Sn, ^{99}Tc, ^{90}Sr and several actinides like ^{239}Pu, ^{241}Am and ^{244}Cm (WHO, 1982). Spent fuel with 4.2 wt.% enrichment in ^{235}U may contain 3.2–8.75 g ^{79}Se t^{-1} after 6 years of cooling (Magill *et al.*, 2003); 3.2 wt.% enriched spent nuclear fuel with a burn-up of 44.9 GWd t^{-1} from a pressurized water reactor (PWR) will produce 5.2 ($\pm$1.5) g ^{79}Se t^{-1} U (Asai *et al.*, 2011). The composition of a high level waste solution recovered after reprocessing a 3.5–4.9 wt.% enriched uranium oxide (UOX) spent fuel from a PWR after 3 y may contain even higher quantities of 77.04–136 g SeO_2 t^{-1} U (i.e., higher than those estimated for In_2O_3, SnO_2, Sb_2O_3, PuO_2, CmO_2, Tb_2O_3, and Dy_2O_3; Caurant *et al.*, 2009). These estimations are still part of ongoing research as they depend on the accuracy of nuclear reaction cross sections. Nevertheless, they are fundamental for understanding the amount of Se expected to be formed within the nuclear fuel cycle and to justify its relevance for research in nuclear waste disposal.

2.4.2 Underground reactivity and dispersion

2.4.2.1 The multi-barrier system: from the fuel to the host rock

Radionuclides in the spent fuel accumulate within the fuel matrix, at the grain boundaries, in the cladding structure or in the gap in between. In general, ^{79}Se is assumed to diffuse out of the fuel grains and migrate to the periphery of the pellets, like other volatile elements such as I and Cs. A considerable part of ^{79}Se in the nuclear fuel accumulates in the gap between the UO_2 pellets and the Zircaloy cladding, or along grain boundaries in the fuel pellets (Johnson & McGinnes, 2002). For instance, a spent fuel from Belgium with an average burn up of 47.3 GWd tHM^{-1} and 4.05% ^{235}U enrichment shows an average distribution of ^{79}Se in Bq per primary waste package of 6.82×10^4 in the structural metals, 6.35×10^6 in the claddings and 9.82×10^8 in the fuel matrix (Yu & Weetjens, 2016).

Nuclear waste is intended to be isolated and contained within a multi-barrier system upon disposal. This multi-barrier consists of both engineered/artificial

retention structures (e.g., waste forms, canisters, buffers, backfills, seals and plugs) and geological/natural materials (e.g., the host rock). Over time and depending on the host rock type, these barriers may become saturated with groundwater and may lose their ability to provide complete containment, thus releasing radionuclides into the environment (Olszewska *et al.*, 2015). In fact, upon contact with groundwater, up to 20% of the ^{79}Se content in the nuclear waste may be released within the 'instant release fraction (IRF)' after canister failure together with ^{36}Cl and ^{129}I (Johnson & McGinnes, 2002; Yu & Weetjens, 2016). The fate of the remaining ^{79}Se will be linked to the solubility of the fuel components over time. This means that long-term ^{79}Se releases will be determined by the dissolution rate of the fuel/cladding matrix (not straightforward to estimate; Yu & Weetjens, 2016). It also implies that a long lifetime of the matrix will cause a long-time spread of ^{79}Se releases at low rates and doses. Short lifetimes of the matrix would favour fast release rates and higher doses.

The transport processes of released radionuclides will follow radionuclide-dependent conditions, initially related to the solubility limits of each elemental oxidation state. Direct measurements in the matrix of spent nuclear fuel samples suggest that Se may be bound to U atoms in selenide (Se(-II)) forms (e.g., case in Switzerland; Curti *et al.*, 2015). Additionally, the intrinsic method of constructing deep geological waste repositories implies an initial entrapment of atmospheric (oxic) conditions. Over time, the oxygen may be consumed by microbial activities (De Cannière *et al.*, 2010) or due to corrosion of the canister material, which may take $\sim 10^4$ y. Such effects eventually result in strongly reducing conditions in the near-field to the nuclear waste. These conditions would favour the presence of reduced species of Se like elemental (Se(0)) and selenide (Se(-II)), which generally have a low solubility. As an example, a simple calculation with 1 μM Se concentration in interstitial water (as defined by Gimmi *et al.*, 2014) at pH 7.28 simulating groundwater conditions in Opalinus clay at 25°C, shows precipitation of Se(0) in reducing conditions (i.e., a decrease in the concentration of the soluble species and in parallel the precipitation of solid species for the case study without Fe, Figure 2.1). The presence of other elements such as S, Fe, Mn, Ca or Sr will also influence the solubility of Se, particularly in highly reducing conditions. Continuing with the previous example, in the presence of 1 mM aqueous Fe, Se will show lower solubility than in the absence of Fe for the same chemical system, favouring the precipitation of solid selenides like ferrosilite (e.g., hashed area in the lower panel, and solid species in the upper panel, in Figure 2.1).

Nevertheless, in the direct vicinity of nuclear waste, radiolytic effects may play a role, that is, water molecules may be split by the emitted radiation from the fuel and produce oxidizing radicals like $OH^{\cdot}$ or peroxo-species like HOOH. These molecules together with other oxidizing species present in the water (e.g., nitrate salts from the nuclear waste; Bleyen *et al.*, 2018) will favour oxidative dissolution from the host phases, thus mobilizing radionuclides. The formation of oxidized species of Se

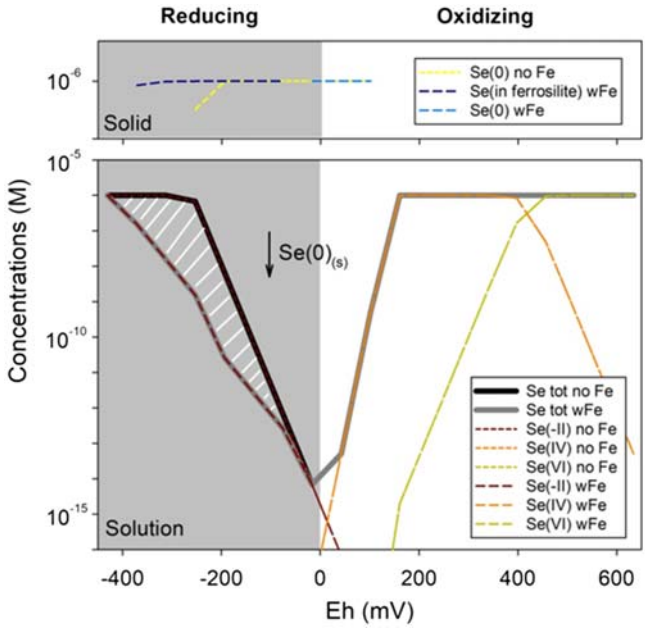

Figure 2.1 Example of the solubility of different Se oxidation states at pH 7.28 for 1 μM total Se content. A comparison between results in the presence (wFe) and without (no Fe) 1 mM aqueous iron is highlighted with a hashed area. Solid species (top panel) and species in solution (bottom panel) are presented. Precipitation of elemental Se is marked with an arrow (bottom panel). Calculations were done with PhreeqC3 (Parkhurst & Appelo, 2013) using the sit.dat (thermochimie) database (Giffaut *et al.*, 2014). The water composition corresponds to that used by Gimmi *et al.* (2014) to simulate groundwater conditions in Opalinus clay at 25°C.

could imply a higher mobility and dispersion than the reduced species, given the high solubility limits of Se(IV) and Se(VI) (e.g., increased concentration of Se in solution, lower panel in Figure 2.1). Nevertheless, oxidizing conditions might not necessarily imply mobilization of Se. For instance, Se(IV) and Se(VI) may also be incorporated into Fe-bearing mineral phases in oxic conditions (e.g., max. 15% retention of Se(VI) and complete uptake of 10^{-3} M of Se(IV) by both adsorption and irreversible co-precipitation during aging of 9.0 g L^{-1} of ferrihydrite into hematite at pH 7.5, or immobilization of 10^{-3} M Se(IV) and Se(VI) at pH 9.2 by co-precipitation with Fe during magnetite formation via Fe(II) hydroxide and green rust; Börsig *et al.*, 2017, 2018).

In any case, a general, inherent gradient between the source and the surrounding environment develops, becoming less reducing from the near-field towards the biosphere. Cementitious systems (e.g., mostly AFm phases, i.e., a family of

hydrated calcium aluminates) as well as bentonite clays (presenting microbially-mediated processes) used within the multi-barrier system at the interface between the nuclear waste and the host rock may retain Se species (e.g., formation of solid solutions mostly for Se(IV) and Se(VI) species; Duro *et al.*, 2020; Ruiz-Fresneda *et al.*, 2018). More detailed information about the multi-barrier system and the interfacial solution chemistry of Se can be found in Abdelouas and Grambow (2012).

2.4.2.2 Reactivity within the host rock: mobility and dispersion of Se species

The extent of the radionuclide transport by groundwater, through advection and/or diffusion, depends on the porosity and permeability of the host rock (i.e., rock salt, clay rock or crystalline rock), the mineralogy of the host rock and on the on-site physico-chemical conditions (e.g., reducing environment with heterogeneous assemblage of minerals and organic phases in the host rock; Altmann, 2008). Case study areas include Boom Clay at Mol (Belgium, e.g., NIROND, 2001), Opalinus clay at Mont Terri and granitic rock at the Grimsel Fels Labor (Switzerland, e.g., Alexander *et al.*, 2009; Bleyen *et al.*, 2018; Eikenberg *et al.*, 1997; Ikonen, 2017), the Asse salt mine (Germany, e.g., Kienzler *et al.*, 2016; Rabung *et al.*, 2018), granitic rock at the Äspö laboratory (Sweden, e.g., TR-99-06), and the Callovo-Oxfordian clay at Bure (France, e.g., Descostes *et al.*, 2008). More information on the underground research infrastructures can be found on the internet (last accessed on the 30th October 2020): https://www.sckcen.be/en/expertises/environment/waste-and-disposal (Belgium), https://www.mont-terri.ch/ and https://www.nagra.ch/de/felslaborgrimsel.htm (Switzerland), https://www.bge.de/de/asse/ (Germany), https://www.skb.com/research-and-technology/laboratories/the-aspo-hard-rock-laboratory/ (Sweden), and https://meusehautemarne.andra.fr/landra-en-meusehaute-marne/installations/le-laboratoire-souterrain (France).

Nevertheless, there is actually little certainty on the true composition of pore waters of host rocks (e.g., Gaucher *et al.*, 2009; Gimmi *et al.*, 2014; Kienzler *et al.*, 2016), or, even more concerning, on the speciation of Se in the pore water of the host rock (e.g., De Cannière *et al.*, 2010; Hoving, 2018). Uncertainties within developed transport models include: (i) specific solubility limits (e.g., from the formation of ferroselite, $FeSe_2$ to the precipitation of Se(0) in strongly reducing conditions; Iida *et al.*, 2009), (ii) the assumption of shared oxidation states due to slow transformation kinetics (e.g., reduction of Se(VI) to lower oxidation states; Grambow, 2008), (iii) the aqueous speciation of Se (e.g., formation of $CaSeO_3$ complexes in solution for Se(IV) in hyperalkaline solutions in contact with cementitious materials or bentonite from the retention structures; Alhajji, 2007; Mace, 2006) or Se adsorption/complexation to other phases (e.g.,

in the presence of organic matter or mineral surfaces), and (iv) the presence or absence of equilibrium conditions (Altmann, 2008).

For instance, existing models assume releases of Se as Se(IV) and Se(VI) oxyanions. However, thermodynamic calculations suggest that Se should be in lower oxidation states (-II and 0) due to interactions with the iron from the canister materials or due to developed reducing conditions within the host rock (e.g., diffusion through clays; Basu *et al.*, 2007; Beauwens *et al.*, 2005; Descostes *et al.*, 2008; Gautschi, 2017). In fact, solid samples containing Se(0) and Se(IV) next to each other originating from reducing environments in Boom Clay have been reported (e.g., Breynaert *et al.*, 2010; Hoving, 2018). Under these conditions, 14–92% of 4–400 mg L^{-1} of Se(IV), respectively, was adsorbed suggesting variable retention mechanisms depending on the Se(IV) concentration in the pore water. Microbially-mediated reactions influencing Se oxidation states within the host rock are also a potential scenario (De Cannière *et al.*, 2010; Ruiz-Fresneda *et al.*, 2018), the cause of which is most likely the high organic matter content mainly present in claystone.

Mobile species migrating through the host rock will be subjected to electrostatic interactions, potentially influencing their diffusion rates. Diffusion may be very low due to anion exclusion in the small, few nanometres pore sizes of claystone where the electric double layers overlap, hindering transport of Se species through the pores (Grambow, 2008). Low anion sorption, on the other hand, is expected in argillaceous rocks due to the electrostatic repulsion developed on the surface, and may favour transport. Conservative approaches usually assume un-retarded transport for all Se species, resulting in a high mobility/dispersion. Clay-Se interactions remain a field of research under development for which electrostatic models can greatly contribute to migration scenarios, particularly within the context of nuclear waste barrier efficiency (e.g., Charlet *et al.*, 2007; Ervanne *et al.*, 2016).

In repositories composed of granite, groundwater will disperse radionuclides relatively rapidly through rock fractures unless retained by diffusion into the rock pores or sorption onto mineral surfaces (Ikonen, 2017; Ikonen *et al.*, 2016). For instance, geological units containing apatite, pyrite and iron oxides may readily immobilize selenite (ANDRA, 2005; Börsig *et al.*, 2017; Hoving, 2018). Effective diffusion coefficients of 2.5 $(\pm 1.5) \times 10^{-12}$ m^2 s^{-1} and 7 $(\pm 2) \times 10^{-13}$ m^2 s^{-1} were obtained for Se in Grimsel granodiorite and Kuru grey granite, respectively (Ikonen, 2017). Sorption interactions between dissolved species and mineral surfaces can be approximated by a solid/liquid partition coefficient (*Kd*). Examples of experimental studies aiming at obtaining representative *Kd* values for nuclear waste repositories are summarized in Table 2.2. Noteworthy, it has been suggested that many *Kd* values used in transport models for underground dispersion of radionuclides may be overestimated if originally based on batch experiments using crushed materials (i.e., potentially not representing proper solid/liquid partitioning along rock cracks, especially in the case of Se; Altmann, 2008; Ikonen, 2017). Enhanced

Table 2.2 Examples of solid/liquid partitioning (*Kd*) values used for radioactive risk assessment of radionuclide mobility in underground and surface environments.

Materials/Conditions	*Kd* (L kg^{-1})	Reference
Applied in nuclear waste near-field conditions		
Crushed quartz in synthetic ground/seawater	<1.0	Lee *et al.* (2012)
Crushed-bentonite in synthetic ground/seawater	10–22	Lee *et al.* (2012)
Mudrock in synthetic ground and seawater	40–80	Lee *et al.* (2008)
Block scale diffusion through granitic rock	0.1–1.5	Ikonen *et al.* (2016)
Crushed granitic rock	6.2–7.0	Ikonen *et al.* (2016)
Solid claystones in reducing environment	~11	Grambow (2008)
Crushed rocks from overburden of Asse salt mine[a]	7–137	Rabung *et al.* (2018)
Applied in surface environmental compartments		
All soils	4.0–2100 (200, $N = 172$)[b]	IAEA TRS 422
Sandy soils	56[b]; 4.0–1600 (56, $N = 15$)[b]	Gil-García *et al.* (2009) IAEA TRS 422
Clay soils	240[b]	Gil-García *et al.* (2009)
Loam + clay soils	12–2100 (220, $N = 134$)[b]	IAEA TRS 422
Organic soils	230–1800 (1000, $N = 2$)[b]	IAEA TRS 422
Average upper crust and ocean water	~100	Grambow (2008)
0.3 ng ^{75}Se L^{-1} added to estuarine SPM[c]	9.0–84.1	Gil-Díaz *et al.* (2020a)
100 μg ^{77}Se L^{-1} added to estuarine SPM[c]	315–630	Gil-Díaz *et al.* (2020b)
SPM of 100 mg L^{-1} in San Francisco Estuary	~100–31 600	Benoit *et al.* (2010)
19 Japanese coastal regions	~400–7900	Takata *et al.* (2016)
Open ocean	1000	IAEA TRS 422
Ocean margin	3000	IAEA TRS 422

[a]Se(IV) in a cocktail solution of radionuclides; [b]Geometric means; [c]SPM concentrations of 10, 100 and 1000 mg L^{-1}.
Abbreviations: SPM, suspended particulate matter.

solubility in natural solids may also be related to the presence of organic complexing agents in the interstitial water (Grambow, 2008). Further understanding of the processes behind sorption of Se on mineral surfaces and *Kd* values can be achieved when the surface site properties and the pore water chemistry are well known and explained by mechanistic models such as surface complexation models (e.g., Davis & Leckie, 1980; Grambow, 2008; Nie *et al.*, 2017). In any case, all *Kd* values are relatively low, suggesting a high mobility of Se and, thus, eventual dispersion into the geologic overburden.

Another process potentially retaining traces of Se species within the host rock is related to its structural incorporation into minerals. For instance, some studies

suggest that ^{79}Se may become immobilized when interacting with uranyl phases present as low concentration impurities in the nuclear fuel waste due to substitution of Si by Se in solid structures of, for example, α-uranophane – $(Ca(UO_2)_2(SiO_3OH)_2 \cdot 5H_2O)$ and boltwoodite – $HK(UO_2)(SiO_4) \cdot 1.5(H_2O)$ (Chen *et al.*, 1999). Others suggest favoured structural incorporation of Se(IV) into calcite, particularly on the surface and potentially in deeper layers upon precipitation at highly supersaturated conditions (Heberling *et al.*, 2014; Polly *et al.*, 2017). The most effective process regarding mineral inclusion could be Se incorporation to Fe-bearing minerals, present as container corrosion products or constituent of host rocks and in bentonite backfills. In fact, studies in this field have shown >98% incorporation of Se(-II) and Se(IV) from 10^{-3} M total Se into pyrite (FeS_2) and mackinawite (FeS) for highly supersaturated solutions under acidic and anoxic conditions (Diener *et al.*, 2012; Finck *et al.*, 2012). Additionally, aging processes such as the transformation of ferrihydrite into hematite and/or Fe(II) hydroxides or green rust into magnetite may efficiently incorporate Se(IV), and in lower quantities Se(VI) (Börsig *et al.*, 2017, 2018).

2.4.2.3 Simulated environmental releases

Radionuclide dispersion scenarios are developed to foresee the long-term consequences of storing nuclear waste underground and to protect future generations from potential environmental releases. These scenarios are based on long-term radioactive risk, as radionuclide releases to the environment are expected between ten thousand and several hundred thousand years. This time frame is related to expected durability of the waste containers and the inherent properties of the long-lived ^{79}Se. It is estimated from conservative approaches as applied in worst case scenarios, that is, independent of the estimated timescales of all the retention mechanisms mentioned in the previous sections: transport subjected to retardation factors as determined by solid/liquid partitioning (Eikenberg *et al.*, 1997; Hampel *et al.*, 2013).

Estimated concentrations in the near-field of nuclear waste repositories could be in the order of 10^{-11} M of ^{79}Se (i.e., <1 ng L^{-1}, with 10^{-9} M of total Se corresponding to ~80 ng L^{-1}; Grambow, 2008). These levels are actually below saturated conditions (*c.f. Section 2.4.2.1*) and will decrease in the far-field from the source. This decrease is also reflected by estimated outgoing fluxes from the deep geological units towards surface environments. For instance, fluxes of ~72 g y^{-1} ^{79}Se from a 10-y aged high-level waste may be expected in the near-field (*c.f. Section 2.4.1*). Preliminary simulations of far-field conditions suggest a maximum flux peak of 2×10^7 Bq y^{-1} (equivalent to ~39 mg y^{-1}; NIROND, 2001) after 150 000–200 000 y into the interface between Boom Clay and a Neogene Aquifer in Belgium. Maximum releases of ~10^{-6} mol ^{79}Se y^{-1} (equivalent to ~79 µg y^{-1}; Altmann, 2008) at around 100 000 y are expected from a model reference claystone geological barrier in the geologic overburden.

These releases lead to effective dose levels which are in general low, compared to environmental activities, as will be discussed in *Section 2.6*. The reported concentrations do not contribute significantly to the environmental budget of Se, or to the local chemotoxicity of Se. These concentrations are below average Se environmental levels (e.g., median 340 ng L^{-1} in European rivers; Salminen *et al.*, 2005) and below the limits of drinking water quality for both total Se (1.3×10^{-7} M, equivalent to ~10 µg L^{-1}) and ^{79}Se (47 Bq L^{-1}, equivalent to ~92 ng L^{-1}; Grambow, 2008). Likewise, reported flux estimates are also very low compared to currently estimated annual fluxes of stable Se from rivers/estuaries subjected to anthropogenic activities into coastal areas. For example, 390 tons y^{-1} have been estimated for the Yangtze River (~3.5 tons y^{-1} ^{74}Se, the least abundant stable isotope of Se; Yao *et al.*, 2007) and ~62000 tons y^{-1} for the Lingdingyang Estuary (~550 tons y^{-1} ^{74}Se; Yao *et al.*, 2006). Nevertheless, better estimations of both far-field ^{79}Se releases and current gross/net environmental fluxes are required to confirm such statements.

2.5 ENVIRONMENTAL DISPERSION SCENARIOS

2.5.1 Conceptual model and assumptions

The main concern in the radioecological risk assessment of ^{79}Se is its transport/remobilization from deep strata and underground waters to surface aquatic and terrestrial systems. A visual diagram is present in Figure 2.2 as an example of a geological setting containing a nuclear waste repository and the environmental compartments involved in the potential transport, dispersion and fate of ^{79}Se from the source to the biosphere and within the biosphere. The presence of ultra-trace levels (or below) of ^{79}Se in natural samples is expected to be subjected to a complex mix of processes (e.g., various oxidation states, precipitation/dissolution and sorption/desorption from various phases). These processes are site-specific, thus, cannot be generalized or expected to be comparable. Nevertheless, most studies agree on the general bioavailability of ^{79}Se, which, however, still depends on the chemical species, as well as the specific organisms and environmental compartments involved (*c.f. Section 2.6*).

Furthermore, differences between the geochemical behaviour of radionuclides and their homologue stable isotopes may exist in specific occasions where recoil effects, mass differences, and radiolytic effects play a role in the system. However, recoil effects are of limited relevance for beta-emitters and radiolytic effects play a role directly next to the waste, not in surface environments where low activities are expected. Isotopic mass effects have been reported for stable Se, as will be discussed below, however, as ^{79}Se is between the most abundant isotopes ^{78}Se and ^{80}Se, mass effects will be small, and likely within the quantification uncertainties of, for example, *Kd* determinations. Therefore, as a general rule, works aiming at understanding the risk assessment of nuclear discharges in surface environments of the geosphere and the biosphere often

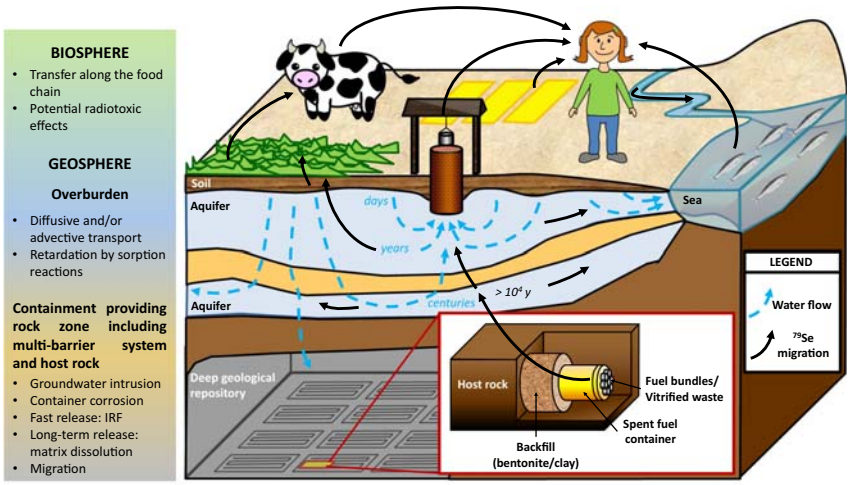

Figure 2.2 Visual scheme to represent the interaction pathways in aquatic and terrestrial systems between potential releases of ^{79}Se from deep geological repositories of spent nuclear fuel (*c.f. Section 2.4*) and accumulation in the biosphere, including ingestion pathways for human uptake (*c.f. Section 2.6*). Examples of the processes involved in each environmental compartment are summarized in the left panel. The geosphere is considered as the geologic underground, while the biosphere includes the pedosphere, the hydrosphere, and (to a limited extent) the atmosphere. Similar schemes should be adapted for site-specific scenarios. Abbreviation: instant release fraction (IRF).

apply the known environmental behaviour of stable Se isotopes as analogues of their radioactive counterparts.

2.5.2 Biogeochemical behaviour in aquatic systems

Once the groundwater has been in contact with the waste repository and is contaminated with ^{79}Se, it may eventually transport ^{79}Se to surface aquatic systems such as rivers and estuaries (e.g., Figure 2.2). In these systems, Se is considered to be relatively mobile, given reported *Kd* values (e.g., Table 2.2). Nevertheless, attention should be paid when extracting conclusions and applying field-based *Kd* values to dispersion and transport models for nuclear risk assessment. In fact, it has been recently suggested that both solid fractionation and *Kd* of added elements to the environment (e.g., anthropogenic releases) may differ from those registered from inherited (geologically-derived) analogue counterparts. The potential added/inherited duality may also be the reason why field- and laboratory-based *Kd* values vary for certain elements in aquatic systems (e.g., Ciceri *et al.*, 1988). Field-based *Kd* values integrate inherited (refractory)

trace elements and laboratory-based *Kd* values address solid/liquid partitioning of spiked elements (better simulating anthropogenic releases). Therefore, reporting proper *Kd* values is of great relevance, particularly from added elements at environmentally representative conditions. Nevertheless, the recommended *Kd* values by the IAEA (IAEA TRS 422) for radionuclide transport models in surface environments are still based indistinctly on experimental or field *Kd* values (e.g., Table 2.2). This may lead to scenarios suggesting a higher particle affinity of added Se compared to expected reactivity in underground conditions.

It is difficult to ascertain if this difference between added and inherent behaviour also applies to Se. This is particularly the case in solid fractionation studies aiming at determining Se solid carrier phases. Indeed, it is difficult to draw sound conclusions from studies where the added chemicals might change the original conditions of the Se species and/or the minerals, inducing a biased behaviour of Se independent of the targeted, operationally-defined carrier phases (e.g., enhanced mobility due to reagents containing organic compounds or a change in the oxidation state of Se; Gil-Díaz *et al.*, 2020b; Gruebel *et al.*, 1988; Lenz *et al.*, 2008). It is also extremely challenging to measure Se in complicated matrices of most of the extraction solutions. Furthermore, isotopically-labelled studies using ^{75}Se radiotracer and/or stable Se do not focus on determining both inherited and added Se, nuancing a more conclusive statement on the matter. One study suggests that, under oxic and abiotic conditions with natural water/sediment matrices, added Se may be more easily exchangeable and mobile during early diagenetic processes than inherited forms (Gil-Díaz *et al.*, 2020b). A further point of interest is to understand what happens to added elements over time. The added Se might be more mobile initially, but over time the question remains whether it could get immobilized more strongly. For environmental scenarios this knowledge and especially the kinetics of such transformations are very important.

In any case, the transport of ^{79}Se in aquatic systems is expected to be mostly in the dissolved phase, thus, subjected to the specific, local biogeochemistry in its soluble forms, which are considered highly to moderately bioavailable (Altmann, 2008). Speciation of Se in natural waters would be expected to involve oxyanion species of Se(IV) and Se(VI) such as $HSeO_3^-$, SeO_3^{2-}, and SeO_4^{2-} in oxidizing conditions at pH >5 (Torres *et al.*, 2011). Other redox states such as Se(-II) and Se(0) may also occur in stagnant waters or in sites dominated by biological activity under reducing conditions (e.g., Wang *et al.*, 2001). Depending on the environmental sites, elemental concentrations, and pH and Eh conditions, interactions with metal ions may occur resulting in cation species such as $[Cu(HSeO_3)]^+$, $[Ca(HSeO_3)]^+$ and $[Mg(HSeO_3)]^+$ at pH >4 (Torres *et al.*, 2011). In any case, this transport in soluble forms would imply a rate of dispersion in surface aquatic systems most likely linked to inherent timescales of hydrological processes (e.g., river discharges, seasonal patterns, and tidal influence). ^{79}Se may also show a more or less important reactivity along the salinity and turbidity gradients of estuarine systems (i.e., conservative vs non-conservative

biogeochemical behaviour) according to the specific continent-ocean transition system involved (e.g., Chang *et al.*, 2016; Cutter, 1989; Measures & Burton, 1978; Seyler & Martin, 1991; van den Berg *et al.*, 1991; van der Sloot *et al.*, 1985; Yao *et al.*, 2006). Given the long half-life of the expected Se radioactive releases, ^{79}Se may eventually reach the ocean and, further, cycle several times within the biogeochemical cycle of Se in accordance with its nutrient-like behaviour (Cutter & Cutter, 1995). Radioactive Se may also transfer to the atmosphere when methylation processes are favoured within estuaries or in the ocean (e.g., Amouroux & Donard, 1997; Feinberg *et al.*, 2020).

2.5.3 Biogeochemical behaviour in terrestrial systems

Contaminated groundwater in terrestrial systems may involve biological uptake by humans from drinking water and/or from food intake due to the direct contact of soils with contaminated groundwater or the use of such groundwater for irrigation (e.g., Figure 2.2). The main factors controlling the speciation and behaviour/mobility of ^{79}Se in soils are redox potential (Eh) and pH soil levels (i.e., classical Eh-pH diagrams), sorption/complexation processes onto inorganic/organic phases (e.g., competition of Se sorption with other anions such as phosphate, introduced by fertilizers; Nothstein *et al.*, 2019), and active biological fixation/transformations (Dhillon & Dhillon, 1991, 2019; Koch-Steindl & Pröhl, 2001; Natasha *et al.*, 2018). Site-specific conditions will be related to the intrinsic characteristics of the soil, the affinity of plants for Se uptake, the climate of the region and soil management, which in turn will determine the daily intake by animals and humans.

Soils may act as long-term secondary sources of radiation when solid adsorption/complexation of ^{79}Se as selenite is favoured and/or in waterlogged systems where precipitation of elemental selenium may occur. For example, reduction reactions may be induced abiotically from heterogeneous reactions with Fe(II)-containing minerals (Février & Martin-Garin, 2005). Soils may also present microenvironments where, for example, reduced species can be formed in soil aggregates even if the soils are considered as totally oxic (Eiche *et al.*, 2015). In oxic conditions, a certain reactivity may be inferred in specific soils (e.g., as seen in *Kd* values, Table 2.2), though a general mobility is also assumed for terrestrial environments, particularly in the presence of other anions in solution such as phosphate (Dhillon & Dhillon, 2019; Gustafsson & Johnsson, 1994).

Nevertheless, soil systems are highly influenced by biological activities, and *Kd* transport models alone may not be sufficient to represent migration in soil horizons, particularly in the presence of microorganisms (Février & Martin-Garin, 2005; Natasha *et al.*, 2018). In fact, an active biotic role such as microbial reduction may significantly enhance immobilization of Se compared to abiotic reduction processes (e.g., >85% of environmentally-relevant spikes of ^{75}Se were incorporated into the low molecular weight organic fraction of forest soils in

<64 h; Darcheville *et al.*, 2008; Gustafsson & Johnsson, 1994). This role is in accordance with solid fractionation studies suggesting a high association of Se with the organic fraction. Furthermore, depending on the location of the deep geological site, released ^{79}Se may also be subjected to complex speciation changes and uptake by plants, characteristic but not exclusively for seleniferous areas (e.g., area of Punjab in India; Eiche *et al.*, 2019). Microorganisms can also produce nano-elemental Se from Se(IV) under relatively oxic conditions (Bajaj *et al.*, 2012). Potential biomethylation processes in soils due to microbial communities would also favour a transfer of radioactive, methylated Se species to the atmosphere (Feinberg *et al.*, 2020), with the consequent dispersion of the corresponding radioactivity (expected to be very low, *Section 2.4.2.3*).

Interestingly, when mobile Se is introduced into the soil through irrigation, it can be easily taken up by plants, where Se may be reduced mainly to organic species (Eiche *et al.*, 2019; Schilling *et al.*, 2015). Depending on the Se concentration (toxicity) or the plant species, some Se might be volatilized. Most importantly, as soon as the plant dies, Se remains in some parts as organic Se within the soil producing a long-term pool. Furthermore, some selenate might be reduced within the soil to selenite which is adsorbed or further reduced into Se(0), which would also lead to an on-site long-term enrichment (Eiche *et al.*, 2019). Consequently, once Se has intruded into a soil-plant system, it can remain there for a long time, especially if the plants are not fully removed during harvest. The behaviour of organic-Se species also differs from that of inorganic forms. Radionuclide dispersion scenarios should consider these implications of the soil-plant system.

In the terrestrial environments, where there is a significant role of the (micro) biosphere, a question arises concerning the effect of potential isotopic fractionation in radionuclide scenarios. In fact, a compromise between released concentrations and molecular weight of ^{79}Se could be expected to interplay with the local, stable isotopes of Se (e.g., ^{79}Se being lighter, though potentially less abundant, than ^{80}Se and ^{82}Se). Evidence in wetland environments suggests that microbial reduction can be subjected to slight isotopic fractionation, favouring transformations of the lighter isotopes (e.g., maximum fractionation of −5.7‰ for ^{80}Se/^{76}Se in a wide range of both added and inherited Se(IV) and Se(VI) concentrations, from 22 µg L^{-1} to 8 mg L^{-1}; Ellis *et al.*, 2003). Microbial reduction of Se(VI) may even show greater isotope fractionation (^{82}Se/^{76}Se from −9.2‰ to −11.8‰) than that of Se(IV) (max. −7.8‰), suggesting different metabolic pathways (Schilling *et al.*, 2020). Surprisingly, though potentially less relevant, this process could also take place during abiotic reduction (e.g., favoured adsorption of the lighter isotopes of Se(IV) onto Fe and Mn oxides, ∼1‰ for ^{82}Se/^{76}Se; Xu *et al.*, 2020). Plants may also selectively uptake Se isotopes, for example, inducing high fractionation of ^{82}Se/^{76}Se of up to +3.5‰ of Se(VI) and +1.9‰ of Se(IV), suggesting an enrichment in heavy isotopes within the plant (Banning *et al.*, 2013, 2018), particularly in irrigated systems (e.g., Schilling *et al.*, 2015). These studies indicate that ^{79}Se may be subject to

isotope fractionation. However, delta values are expected to be closer to zero compared to the extreme isotope pairs $^{82}Se/^{76}Se$ or $^{80}Se/^{76}Se$.

Furthermore, dispersion scenarios in terrestrial systems are based on the current knowledge of site-specific soil conditions and known physico-chemical/biological processes. However, ideally future changes in the organic matter content and quality of soils (happening within decades to centuries) and changes in weathering and pedogenesis (occurring within millennia; Dhillon & Dhillon, 2019; Koch-Steindl & Pröhl, 2001) should be included in risk assessment scenarios as they fall within the timescales of the half-life of ^{79}Se. Additionally, potentially forthcoming changing conditions and their consequences (e.g., climate change and future soil management) should also be taken into account. Important aspects also include irrigation, introducing Se but also potentially leading to salinization; industry bringing in anthropogenic molecules, which might be very persistent; and heavy rain, washing out Se or leading to water-logged intervals. A summary of contrasting examples of climatic scenarios and potential impacts in soil processes concerning Se are described in Koch-Steindl and Pröhl (2001) and a more recent case scenario predicting site-specific trends of future Se in soils worldwide can be found in Jones *et al.* (2017). For instance, an increase in temperature, precipitation and positive water balance could accelerate all soil processes and favour soil leaching, low pH and higher turnover of organic matter, all of which could lead to an increased mobilization of Se. This would enhance the bioavailability of ^{79}Se for the local biosphere (both microorganisms as well as plant uptake) and/or its transport to underground water systems. In arid environments, high temperatures may slow down organic matter decomposition and mineral weathering, decreasing the mobilization of radionuclides attached/sorbed to such particles. Increased erosion by wind and water in both future arid and humid conditions may favour the spatial distribution of radionuclides (higher dispersion, less concentrated on-site).

2.6 IMPACT OF RADIOACTIVE Se ON THE BIOSPHERE: INSIGHTS FROM ECOLOGICAL MODELS

2.6.1 Bioaccumulation factors in aquatic and terrestrial systems

There are several mathematical approaches used to simulate the biological uptake and acute/chronic accumulation of trace elements in different environmental compartments. These are essential tools for predicting worst-case scenarios of potential intake of radionuclides into the biosphere in order to develop management strategies to protect the environment and humans, especially concerning potential external and internal exposure doses. This is particularly important for radionuclide risk assessment where direct measurements are not always available due to the lack of environmental evidence (e.g., case of ^{79}Se).

These models quantify the uptake of radionuclides by organisms through concentration factors or bioaccumulation factors, and include the dynamic transfer/retention within the organisms by taking into account the biological half-lives of the elements (Beresford *et al.*, 2015). Concentration factors account for the relative concentration/activity of the radionuclide in the organism compared to that present in the water (direct pathway) and/or the food (trophic pathway).

Existing wildlife projects/models for risk assessment and management of ionizing radiation as well as α/β-emitters (e.g., the ERICA/FREDERICA Tool, the Ecopath-with-Ecosim model, the ENVIRHOM Program; Beresford *et al.*, 2008; Booth *et al.*, 2020; Henner, 2008; Hosseini *et al.*, 2008) mostly rely on databases composed of known concentration factors from both field and experimental conditions. Current databases show elevated concentration factors for Se in many trophic levels of both aquatic and terrestrial organisms (Table 2.3). Indeed, other radionuclides of radioecological relevance show lower intakes. Such is the case for the 'geochemical pair' of Se, Te (e.g., <700 L kg^{-1} in aquatic and <1 L kg^{-1} in terrestrial systems), or the commonly followed ^{137}Cs and ^{131}I (e.g., $\sim10^{2}$–10^{3} L kg^{-1} in the aquatic and $\sim10^{-2}$ L kg^{-1} in the terrestrial system; Gil-Díaz, 2019). As expected, biomagnification patterns for Se can also be discerned from these databases, particularly in marine environments (Table 2.3). This means that, despite the expected, low environmental activities of ^{79}Se reaching the aquatic and terrestrial systems, organisms may accumulate ^{79}Se and transfer it along the trophic chain. Nevertheless, these databases still require further research regarding the assessment of ^{79}Se as, for instance, there are few studied groups in freshwater and brackish systems, occasionally equal concentration factors are applied to different groups, and there are generally high standard deviations, when specified (Table 2.3).

2.6.2 Human radiotoxicity: exposure pathways and estimated doses

Within the aim of providing dose rates in realistic scenarios, important advancements in radioecological studies have been achieved. Particularly after the Fukushima Dai-ichi NPP accidental event, improvements in post-accidental assessment were made in marine ecosystems for commonly followed radionuclides, which have not yet been applied for ^{79}Se (Beresford *et al.*, 2015; Booth *et al.*, 2020; Vives i Batlle *et al.*, 2018). Nevertheless, terrestrial models including a comprehensive view of both element-dependent parameters (e.g., transfer factors and soil-plant distribution coefficients) and element-independent parameters (e.g., irrigation, agricultural practices and human consumption rates) have been developed and applied for ^{79}Se. For instance, the BIOGEM model was used to identify the main exposure doses for humans at five national geological repositories (e.g., Kowe *et al.*, 2005). Results suggested that, in general, the

Table 2.3 Recommended concentration factors of Se used for radionuclide risk assessment in aquatic and terrestrial organisms.

Organisms	Conditions	Concentration factor (L kg^{-1})	Reference
Freshwater			
Zooplankton	*In situ*	6600 ± 3900 (f.w.) ($N = 3$)	IAEA TRS 479
Macroalgae	*In situ*	3100 ± 1300 (f.w.) ($N = 3$)	IAEA TRS 479
Vascular plants	*Ex situ* *In situ*	1000 (f.w.) ($N = 1$) 220 ± 57 (f.w.) ($N = 3$)	Hosseini *et al.* (2008) IAEA TRS 479
Molluscs (Gastropods)	*In situ*	3200 ± 2900 (f.w.) ($N = 3$)	IAEA TRS 479
Fish Benthic feeding Piscivorous	*In situ* *In situ* *In situ*	4800 ± 3300 (f.w.) ($N = 127$) 6200 ± 3700 (f.w.) ($N = 51$) 4200 ± 2700 (f.w.) ($N = 70$)	IAEA TRS 479 IAEA TRS 479 IAEA TRS 479
Insect larvae	*In situ*	2400 ± 1900 (f.w.) ($N = 9$)	IAEA TRS 479
Amphibians	—	63.2 (f.w.) ($N = 1$)	Beresford *et al.* (2008)
Reptiles	*In situ*	2700 ± 2500 (f.w.) ($N = 11$)	IAEA TRS 479
Brackish			
Vascular plants	*In situ*	4200 ± 1000 (f.w.) ($N = 3$)	IAEA TRS 479
Fish	*In situ*	2300 ± 2900 (f.w.) ($N = 8$)	IAEA TRS 479

Marine

Phytoplankton	*In situ*	30000	IAEA TRS 422
	Ex situ	3600 ± 13000 (f.w.) ($N = 94$)	Hosseini *et al.* (2008)
Zooplankton	*In situ*	6000 (f.w.)	IAEA TRS 422
Macroalgae	*In situ*	1000 (f.w.)	IAEA TRS 422
	In situ	430 ± 790 (f.w.) ($N = 36$)	IAEA TRS 479
	In situ	310 ± 300 (f.w.) ($N = 35$)	Hosseini *et al.*, (2008)
Annelids (worms)	*Ex situ*	4500 (f.w.) ($N = 1$)	Hosseini *et al.* (2008)
Cnidaria (anemones)	*Ex situ*	10 (f.w.) ($N = 1$)	Hosseini *et al.* (2008)
Bivalves	*Ex situ*	5000 ± 3700 (f.w.) ($N = 3$)	Hosseini *et al.* (2008)
Gastropods	*In situ*	34.7 ± 31.2 (f.w.) ($N = 7$)	Beresford *et al.* (2008)
Molluscs *(general)*	*In situ*	9000 (d.w.)	IAEA TRS 422
	Ex situ/*In situ*	6700 ± 4600 (f.w.) ($N = 4$)	IAEA TRS 479
Crustaceans	*In situ*	10000 (f.w.)	IAEA TRS 422
	Ex situ/*In situ*	7100 ± 4800 (f.w.) ($N = 4$)	Hosseini *et al.*, (2008)
Fish	*In situ*	10000 (f.w.)	IAEA TRS 422
	Ex situ/*In situ*	9300 ± 4600 (f.w.) ($N = 3$)	Hosseini *et al.* (2008)
Mammals (general)	*In situ*	8300 ± 2700 (f.w.) ($N = 720$)	Hosseini *et al.* (2008)
Pinnipeds (seals and sea lions)	*In situ*	10000 muscle 700000 liver	IAEA TRS 422
Polar bears	*In situ*	8000 muscle 100000 liver	IAEA TRS 422
Cetaceans (whales, dolphins and porpoises)	*In situ*	80000 muscle 400000 liver	IAEA TRS 422

(*Continued*)

Table 2.3 Recommended concentration factors of Se used for radionuclide risk assessment in aquatic and terrestrial organisms (*Continued*).

Organisms	Conditions	Concentration factor (L kg^{-1})	Reference
Terrestrial*			
Grasses and herbs	*In situ*	1.0 ± 2.1 ($N = 364$)	IAEA TRS 479
Grasses	*In situ*	1.8 ± 1.6 ($N = 48$)	IAEA TRS 479
Herbs	*In situ*	1.4 ± 2.2 ($N = 132$)	IAEA TRS 479
Lichen and Bryophytes	*Ex situ*	20 ($N = 1$)	Beresford *et al.* (2008)
		0.36 ± 0.20 ($N = 18$)	IAEA TRS 479
Shrubs	*In situ*	1.81 ± 1.40 ($N = 73$)	Beresford *et al.* (2008)
	In situ	1.5 ± 1.4 ($N = 94$)	IAEA TRS 479
Trees	*In situ*	1.81 ± 1.40 ($N = 73$)	Beresford *et al.* (2008)
Detritivorous invertebrates	–	1.48 ($N = 1$)	Beresford *et al.* (2008)
Soil invertebrates	–	1.48	Beresford *et al.* (2008)
Annelids	–	1.50 ($N = 1$)	IAEA TRS 479
Molluscs (Gastropods)	*In situ*	0.035 ± 0.031 ($N = 7$)	IAEA TRS 479
Reptiles and mammals	*In situ*	0.0632 ± 0.381 ($N = 12$)	Beresford *et al.* (2008)

These values are based on experimental setups (*ex situ)* and/or from environmental sites (*in situ*, from exposure to stable Se). Arithmetic averages and standard deviations (SD), number of samples (N) and fresh weight (f.w.) vs dry weight (d.w.) values are specified when provided by the original reference.

*Resulting units are kg of dry soil per kg of fresh weight of organism.

ingestion pathway is the dominating exposure route, particularly from drinking water and food intake, related to national consumption habits.

It is difficult to precisely estimate the exposure doses from direct intake of drinking water due to the site-specific conditions of each geological repository and the nearby land use. For instance, estimated dose rates for a potential contaminated well 20 km away from a given repository could start showing detectable exposures to ^{79}Se after ~35000 y and reach maximum values of 0.1 mSv y^{-1} after 100000 y (Magill *et al.*, 2003). This dose rate is actually equal to the total admissible effective dose allowed to be discharged from NPPs in liquid and gas releases. It is also of the same order of magnitude as the world average dose of 0.3 mSv y^{-1} for ingestion of natural radionuclides, and below the admissible average doses of ~1 mSv y^{-1} for exposure of the population to background radiation. These comparisons imply a significant, but still acceptable exposure from drinking water for this specific example, though not generalizable and highly dependent on the specific case study. The impact of such estimations could reach doses of concern depending on the activities released from the waste repository and the annual intake of water. More refined predictions are still required as the potential doses of mobile nuclides such as Se are generally largely overestimated due to all the conservative assumptions related to lack of knowledge (Grambow, 2008).

Concerning food consumption, examples of known transfer factors of Se for human consumption of poultry, milk and eggs can be found in IAEA TRS 472. Examples of simulations calculating the radiation effect of ^{79}Se in humans from contaminated seafood suggest non-negligible dose coefficients, particularly from fish (1.7×10^{-7} Sv m^3 kg^{-1} Bq^{-1}), crustaceans (1.4×10^{-7} Sv m^3 kg^{-1} Bq^{-1}), molluscs (1.7×10^{-7} Sv m^3 kg^{-1} Bq^{-1}) and algae (2.8×10^{-8} Sv m^3 kg^{-1} Bq^{-1}). These dose coefficients are comparable to estimations for ^{60}Co, ^{119m}Sn, ^{121m}Sn, ^{129}I, ^{131}I, ^{226}Ra, ^{227}Ac, ^{232}Th, ^{242}Pu and ^{242m}Am (Ganul *et al.*, 2006). These values are higher than the recommended values for ingestion pathways from the International Commission on Radiation Protection (ICRP) using human internal dose conversion factors for ^{79}Se of 2.0×10^{-9}–2.3×10^{-9} Sv Bq^{-1} (Palattao *et al.*, 1997). They are also higher than the effective dose allowed for public ingestion of ^{79}Se, ranging between 1.9×10^{-8}–4.9×10^{-8} Sv Bq^{-1} (Decree 783/2001). In these simulations, intakes of ^{79}Se could reach levels of significant concern in specific conditions. In specific scenarios for solubility limited releases of radionuclides from a high-level nuclear waste repository in Belgian Boom Clay, dose rates related to ^{79}Se were $<10^{-5}$ Sv y^{-1} (e.g., from vitrified waste and spent fuel after >150000 y; Hoving, 2018; NIROND, 2001; Yu & Weetjens, 2016). Estimated internal doses for CANDU fuel in a conceptual clay-based backfill and a plutonic host rock are much lower, falling in the range of 10^{-11}–10^{-7} Sv y^{-1} (e.g. Johnson *et al.*, 1996). Therefore, further research should aim at reducing conservative assumptions in order to proceed towards more realistic descriptions of the Se distribution in the environment.

This knowledge should serve to locate optimal disposal sites and waste management strategies.

Concerning external exposure routes due to proximity to radioactive releases, simulated maximum annual doses for ^{79}Se vary depending on the fuel type, the host rock, and the environmental scenario considered. For granite rock repositories in Sweden, the annual dose of ^{79}Se to the geosphere has been shown to be four orders of magnitude below the local annual limit of 0.15 mSv (TR-99-06). In general, external exposure routes of ^{79}Se are not expected to be critical, though the chemistry of Se in these simulations still has to be refined.

2.7 CONCLUSIONS

Selenium is known to show a mobility and bioavailability in the environment which is dependent on the chemical species. The only radioactive isotope of concern for the environment (^{79}Se) is expected to be released in the long-term ($>10^4$ y) from deep geological nuclear waste repository sites in relatively low concentrations. These radioactive releases may be subjected to more or less complex transformations, showing a characteristic, site-specific behaviour according to the multiple chemical forms in which Se may exist in each environmental compartment. Dispersion scenarios for nuclear risk assessment are still developing and require the complementary information provided by environmental studies on stable Se and experimental studies using stable Se or benefiting from use of the radiotracer, ^{75}Se. Existing analytical challenges such as polyatomic and isobaric interferences encountered when quantifying stable isotopes of Se in environmental samples may be overcome more easily nowadays with new generation ICP-MS. Biological studies suggest a potentially relevant intake of Se by organisms, particularly in aquatic systems. In any case, the incorporation of ^{79}Se into the biogeochemical cycle of Se implies that, in the far future the highest radioactive doses to humans are expected to be linked to internal exposure pathways, whereas the external exposure pathway will contribute with very low doses of ^{79}Se, eventually becoming part of the environmental radioactive background.

REFERENCES

Abdelouas A. and Grambow B. (2012). Aquatic chemistry of long-lived mobile fission and activation products in the context of deep geological disposal. In: Radionuclide Behaviour in the Natural Environment, C. Poinssot and H. Geckeis (eds.), Woodhead Publishing, pp. 70–102.

Aguerre S. and Frechou C. (2006). Development of a radiochemical separation for selenium with the aim of measuring its isotope 79 in low and intermediate nuclear wastes by ICP-MS. *Talanta*, **69**(3), 565–571.

Alexander W. R., Frieg B., Ota K. and Bedrock Geosciences A. (2009). Grimsel test site investigation Phase IV. The Nagra-JAEA in situ study of safety relevant radionuclide

retardation in fractured crystalline rock. III: The RRP project final report (No. NTB--00-07). Bedrock Geosciences.

Alhajji E. (2007). Etude des propriétés de sorption de la bentonite mx-80 vis-à-vis de se (iv), ni (ii) et cs (i). du système disperse au système compacte. Doctoral dissertation, Paris, 11.

Altmann S. (2008). 'Geo'chemical research: a key building block for nuclear waste disposal safety cases. *Journal of Contaminant Hydrology*, **102**(3–4), 174–179.

Amouroux D. and Donard O. F. (1997). Evasion of selenium to the atmosphere via biomethylation processes in the Gironde estuary, France. *Marine Chemistry*, **58**(1–2), 173–188.

ANDRA (2005). Dossier 2005 Argile. Evaluation de sureté du stockage géologique. Agence National pour la gestion des Déchets Radioactifs, Paris.

Araie H., Suzuki I. and Shiraiwa Y. (2008). Identification and characterization of a selenoprotein, thioredoxin reductase, in a unicellular marine haptophyte alga, *Emiliania huxleyi*. *Journal of Biological Chemistry*, **283**(51), 35329–35336.

Arnold R., Augier C., Baker J., Barabash A. S., Basharina-Freshville A., Bongrand M., Brudanin V., Caffrey A. J., Cebrián S., Chapon A. and Chauveau E. (2010). Probing new physics models of neutrinoless double beta decay with SuperNEMO. *The European Physical Journal C*, **70**(4), 927–943.

Artusa D. R., Balzoni A., Beeman J. W., Bellini F., Biassoni M., Brofferio C., Camacho A., Capelli S., Cardani L., Carniti P. and Casali N. (2017). The LUCIFER/CUPID-0 demonstrator: searching for the neutrinoless double-beta decay with Zn 82 Se scintillating bolometers. *Journal of Physics: Conference Series*, **888**(1), 012077.

Asai S., Hanzawa Y., Okumura K., Shinohara N., Inagawa J., Hotoku S., Suzuki K. and Kaneko S. (2011). Determination of ^{79}Se and ^{135}Cs in spent nuclear fuel for inventory estimation of high-level radioactive wastes. *Journal of Nuclear Science and Technology*, **48**(5), 851–854.

Audi G., Bersillon O., Blachot J. and Wapstra A. H. (2003). The NUBASE evaluation of nuclear and decay properties. *Nuclear Physics A*, **624**, 1–124.

Bajaj M., Schmidt S. and Winter J. (2012). Formation of Se (0) Nanoparticles by Duganella sp. and *Agrobacterium* sp. isolated from Se-laden soil of North-East Punjab, India. *Microbial Cell Factories*, **11**(1), 64.

Banning H. M., Stelling M., Eiche E., Nothstein A. K., Neumann T., Schoenberg R., Riemann M. and Nick P. (2013). Use of stable isotope signatures in plants as a tool to explore the selenium cycle in the 'critical zone'. *Selenium in the Environment and Human Health*, **22**, 22–23.

Banning H., Stelling M., König S., Schoenberg R. and Neumann T. (2018). Preparation and purification of organic samples for selenium isotope studies. *PloS One*, **13**(3), e0193826.

Barnekow U., Fesenko S., Kashparov V., Kis-Benedek G., Matisoff G., Onda Y., Sanzharova N., Tarjan S., Tyler A. and Varga B. (2019). Guidelines on Soil and Vegetation Sampling for Radiological Monitoring. International Atomic Energy Agency: Vienna, Austria.

Basu R., Haque S. E., Tang J., Ji J. and Johannesson K. H. (2007). Evolution of selenium concentrations and speciation in groundwater flow systems: Upper Floridan (Florida) and Carrizo Sand (Texas) aquifers. *Chemical Geology*, **246**(3–4), 147–169.

Beaudette D. E., Stupi L. K., Swarowsky A., O'Geen A. T., Chang J. F. and Gallagher B. (2009). Watershed-scale geochemical inventory of soils by portable x-ray fluorescence. *AGUFM*, **2009**, B11A-0467.

Beauwens T., De Cannière P., Moors H., Wang L. and Maes N. (2005). Studying the migration behaviour of selenate in Boom Clay by electromigration. *Engineering Geology*, **77**(3–4), 285–293.

Beilstein M. A. and Whanger P. D. (1988). Glutathione peroxidase activity and chemical forms of selenium in tissues of rats given selenite or selenomethionine. *Journal of Inorganic Biochemistry*, **33**(1), 31–46.

Benoit M. D., Kudela R. M. and Flegal A. R. (2010). Modeled trace element concentrations and partitioning in the San Francisco estuary, based on suspended solids concentration. *Environmental Science and Technology*, **44**(15), 5956–5963.

Beresford N. A., Barnett C. L., Howard B. J., Scott W. A., Brown J. E. and Copplestone D. (2008). Derivation of transfer parameters for use within the ERICA Tool and the default concentration ratios for terrestrial biota. *Journal of Environmental Radioactivity*, **99**(9), 1393–1407.

Beresford N. A., Beaugelin-Seiller K., Burgos J., Cujic M., Fesenko S., Kryshev A., Pachal N., Real A., Su B. S., Tagami K. and Vives i Batlle J. (2015). Radionuclide biological half-life values for terrestrial and aquatic wildlife. *Journal of Environmental Radioactivity*, **150**, 270–276.

Bleyen N., Smets S., Small J., Moors H., Leys N., Albrecht A., De Cannière P., Schwyn B., Wittebroodt C. and Valcke E. (2018). Impact of the electron donor on in situ microbial nitrate reduction in Opalinus Clay: results from the Mont Terri rock laboratory (Switzerland). In: Mont Terri Rock Laboratory, 20 Years. Swiss Journal of Geosciences Supplement, P. Bossart and A. Milnes (eds.), Birkhäuser, Cham, vol. **5**.

Booth S., Walters W. J., Steenbeek J., Christensen V. and Charmasson S. (2020). An Ecopath with Ecosim model for the Pacific coast of eastern Japan: describing the marine environment and its fisheries prior to the Great East Japan earthquake. *Ecological Modelling*, **428**, 109087.

Börsig N., Scheinost A. C., Shaw S., Schild D. and Neumann T. (2017). Uptake mechanisms of selenium oxyanions during the ferrihydrite-hematite recrystallization. *Geochimica et Cosmochimica Acta*, **206**, 236–253.

Börsig N., Scheinost A. C., Shaw S., Schild D. and Neumann T. (2018). Retention and multiphase transformation of selenium oxyanions during the formation of magnetite via iron (II) hydroxide and green rust. *Dalton Transactions*, **47**(32), 11002–11015.

Breynaert E., Scheinost A. C., Dom D., Rossberg A., Vancluysen J., Gobechiya E., Kirschhock C. E. and Maes A. (2010). Reduction of Se (IV) in boom clay: XAS solid phase speciation. *Environmental Science and Technology*, **44**(17), 6649–6655.

Campbell A. D. (1992). A critical survey of hydride generation techniques in atomic spectroscopy (Technical Report). *Pure and Applied Chemistry*, **64**(2), 227–244.

Caurant D., Loiseau P., Majerus O., Aubin-Chevaldonnet V., Bardez I. and Quintas A. (2009). Glasses, Glass-Ceramics and Ceramics for Immobilization of Highly Radioactive Nuclear Wastes. Nova Science, Hauppauge.

Chang Y., Zhang J., Qu J., Zhang G., Zhang A. and Zhang R. (2016). The behavior of dissolved inorganic selenium in the Changjiang Estuary. *Journal of Marine Systems*, **154**, 110–121.

Charlet L., Scheinost A. C., Tournassat C., Greneche J. M., Géhin A., Fernández-Martı A., Coudert S., Tisserand D. and Brendle J. (2007). Electron transfer at the mineral/water interface: selenium reduction by ferrous iron sorbed on clay. *Geochimica et Cosmochimica Acta*, **71**(23), 5731–5749.

Chen F., Burns P. C. and Ewing R. C. (1999). 79Se: geochemical and crystallo-chemical retardation mechanisms. *Journal of Nuclear Materials*, **275**(1), 81–94.

Ciceri G., Traversi A. L., Martinotti W. and Queirazza G. (1988). Radionuclide partitioning between water and suspended matter: comparison of different methodologies. In: Studies in Environmental Science, L. Pawlowski, E. Mentasti, W. J. Lacy and C. Sarzanini (eds.), Elsevier, Vol. **34**, pp. 353–375.

Curti E., Puranen A., Grolimund D., Jädernas D., Sheptyakov D. and Mesbah A. (2015). Characterization of selenium in UO_2 spent nuclear fuel by micro X-ray absorption spectroscopy and its thermodynamic stability. *Environmental Science: Processes and Impacts*, **17**(10), 1760–1768.

Cutter G. A. (1989). The estuarine behaviour of selenium in San Francisco Bay. *Estuarine, Coastal and Shelf Science*, **28**(1), 13–34.

Cutter G. A. and Cutter L. S. (1995). Behavior of dissolved antimony, arsenic, and selenium in the Atlantic Ocean. *Marine Chemistry*, **49**(4), 295–306.

Darcheville O., Février L., Haichar F. Z., Berge O., Martin-Garin A. and Renault P. (2008). Aqueous, solid and gaseous partitioning of selenium in an oxic sandy soil under different microbiological states. *Journal of Environmental Radioactivity*, **99**(6), 981–992.

Dardenne K., González-Robles E., Rothe J., Müller N., Christill G., Lemmer D., Praetorius R., Kienzler B., Metz V., Roth G. and Geckeis H. (2015). XAS and XRF investigation of an actual HAWC glass fragment obtained from the Karlsruhe vitrification plant (VEK). *Journal of Nuclear Materials*, **460**, 209–215.

Davis J. A. and Leckie J. O. (1980). Surface ionization and complexation at the oxide/water interface. 3. Adsorption of anions. *Journal of Colloid and Interface Science*, **74**(1), 32–43.

De Cannière P., Maes A., Williams S., Bruggeman C., Beauwens T., Maes N. and Cowper M. (2010). Behaviour of selenium in Boom Clay. External Report, SCK• CEN-ER-120.

Decree R. (2001). Real Decreto 783/2001, de 6 de julio por el que se aprueba el Reglamento sobre Protección Sanitaria contra Radiaciones Ionizantes.

Descostes M., Blin V., Bazer-Bachi F., Meier P., Grenut B., Radwan J., Schlegel M. L., Buschaert S., Coelho D. and Tevissen E. (2008). Diffusion of anionic species in Callovo-Oxfordian argillites and Oxfordian limestones (Meuse/Haute–Marne, France). *Applied Geochemistry*, **23**(4), 655–677.

Devi P., Jain R., Thakur A., Kumar M., Labhsetwar N. K., Nayak M. and Kumar P. (2017). A systematic review and meta-analysis of voltammetric and optical techniques for inorganic selenium determination in water. *TrAC Trends in Analytical Chemistry*, **95**, 69–85.

Dhillon K. S. and Dhillon S. K. (1991). Selenium toxicity in soils, plants and animals in some parts of Punjab, India. *International Journal of Environmental Studies*, **37**(1–2), 15–24.

Dhillon K. S. and Dhillon S. K. (2019). Genesis of seleniferous soils and associated animal and human health problems. In: Advances in Agronomy, D. L. Sparks (ed.), Academic Press, Vol. **154**, pp. 1–80.

Diener A., Neumann T., Kramar U. and Schild D. (2012). Structure of selenium incorporated in pyrite and mackinawite as determined by XAFS analyses. *Journal of Contaminant Hydrology*, **133**, 30–39.

Dočekal B., Dědina J. and Krivan V. (1997). Radiotracer investigation of hydride trapping efficiency within a graphite furnace. *Spectrochimica Acta Part B: Atomic Spectroscopy*, **52**(6), 787–794.

Duro L., Altmaier M., Holt E., Mäder U., Claret F., Grambow B., Idiart A., Valls A. and Montoya V. (2020). Contribution of the results of the CEBAMA project to decrease uncertainties in the Safety Case and Performance Assessment of radioactive waste repositories. *Applied Geochemistry*, **112**, 104479.

Eiche E., Bardelli F., Nothstein A. K., Charlet L., Göttlicher J., Steininger R., Dhillon K. S. and Sadana U. S. (2015). Selenium distribution and speciation in plant parts of wheat (*Triticum aestivum*) and Indian mustard (*Brassica juncea*) from a seleniferous area of Punjab, India. *Science of the Total Environment*, **505**, 952–961.

Eiche E., Nothstein A. K., Göttlicher J., Steininger R., Dhillon K. S. and Neumann T. (2019). The behaviour of irrigation induced Se in the groundwater-soil-plant system in Punjab, *India. Environmental Science: Processes & Impacts*, **21**(6), 957–969.

Eikenberg J., Ruethi M., Alexander W. R., Frieg B. and Fierz T. (1997). The excavation project in the grimsel test site: in situ high-resolution gamma and alpha spectrometry of ^{60}Co, ^{75}Se, ^{113}Sn, ^{152}Eu, ^{235}U, and ^{237}Np/^{233} Pa. MRS Online Proceedings Library Archive, 506.

Einoder L. D., MacLeod C. K. and Coughanowr C. (2018). Metal and isotope analysis of bird feathers in a contaminated estuary reveals bioaccumulation, biomagnification, and potential toxic effects. *Archives of Environmental Contamination and Toxicology*, **75** (1), 96–110.

Ellis A. S., Johnson T. M., Herbel M. J. and Bullen T. D. (2003). Stable isotope fractionation of selenium by natural microbial consortia. *Chemical Geology*, **195**(1–4), 119–129.

Ervanne H., Hakanen M. and Lehto J. (2016). Selenium sorption on clays in synthetic groundwaters representing crystalline bedrock conditions. *Journal of Radioanalytical and Nuclear Chemistry*, **307**(2), 1365–1373.

Ezoe K., Ohyama S., Hashem M. A., Ohira S. I. and Toda K. (2016). Automated determinations of selenium in thermal power plant wastewater by sequential hydride generation and chemiluminescence detection. *Talanta*, **148**, 609–616.

Feinberg A., Maliki M., Stenke A., Sudret B., Peter T. and Winkel L. H. (2020). Mapping the drivers of uncertainty in atmospheric selenium deposition with global sensitivity analysis. *Atmospheric Chemistry and Physics*, **20**(3), 1363–1390.

Février L. and Martin-Garin A. (2005). Biogeochemical behaviour of anionic radionuclides in soil: Evidence for biotic interactions. *Radioprotection*, **40**(1), S79.

Finck N., Dardenne K., Bosbach D. and Geckeis H. (2012). Selenide retention by mackinawite. *Environmental Science and Technology*, **46**(18), 10004–10011.

Fleming D. E., Groves J. W., Gherase M. R., George G. N., Pickering I. J., Ponomarenko O., Langan G., Spallholz J. E., Alauddin M., Ahsan H. and Ahmed S. (2015). Soft tissue measurement of arsenic and selenium in an animal model using portable X-ray fluorescence. *Radiation Physics and Chemistry*, **116**, 241–247.

Fowler S. W., Teyssie J. L., Acosta A., Gattuso J. P. and Jaubert J. (1999). Radiotracer studies on radionuclide and trace element cycling in corals (No. IAEA-TECDOC--1094).

Fresneda M. A. R., Martín J. D., Bolívar J. G., Cantos M. V. F., Bosch-Estévez G., Moreno M. F. M. and Merroun M. L. (2018). Green synthesis and biotransformation of amorphous Se nanospheres to trigonal 1D Se nanostructures: impact on Se mobility within the concept of radioactive waste disposal. *Environmental Science: Nano*, **5**(9), 2103–2116.

Galinha C., Freitas M. C., Pacheco A. M. G., Coutinho J., Maçãs B. and Almeida A. S. (2012). Radiotracing selenium in bread-wheat seeds for a Se-biofortification program: an optimization study in seed enrichment. *Journal of Radioanalytical and Nuclear Chemistry*, **291**(1), 193–195.

Ganul M. N., Kuchin N. L. and Sergeev I. V. (2006). Prediction of the radiation effect resulting from the contamination of water in marine fisheries. *Atomic Energy*, **100**(2), 79–82.

Gaucher E. C., Tournassat C., Pearson F. J., Blanc P., Crouzet C., Lerouge C. and Altmann S. (2009). A robust model for pore-water chemistry of clayrock. *Geochimica et Cosmochimica Acta*, **73**(21), 6470–6487.

Gautschi A. (2017). Safety-relevant hydrogeological properties of the claystone barrier of a Swiss radioactive waste repository: an evaluation using multiple lines of evidence. *Grundwasser*, **22**(3), 221–233.

Giffaut E., Grivé M., Blanc P., Vieillard P., Colàs E., Gailhanou H., Gaboreau S., Marty N., Made B. and Duro L. (2014). Andra thermodynamic database for performance assessment: ThermoChimie. *Applied Geochemistry*, **49**, 225–236.

Gil-Díaz T. (2019). Tellurium radionuclides produced by major accidental events in nuclear power plants. *Environmental Chemistry*, **16**(4), 296–302.

Gil-Díaz T., Heberling F., Keller V., Fuss M., Böttle M., Eiche E. and Schäfer J. (2020a). Tin-113 and Selenium-75 radiotracer adsorption and desorption kinetics in contrasting estuarine salinity and turbidity conditions. *Journal of Environmental Radioactivity*, **213**, 106133.

Gil-Díaz T., Schäfer J., Keller V., Eiche E., Dutruch L., Mößner C., Lenz M. and Eyrolle F. (2020b). Tellurium and selenium sorption kinetics and solid fractionation under contrasting estuarine salinity and turbidity conditions. *Chemical Geology*, **532**, 119370.

Gil-García C., Tagami K., Uchida S., Rigol A. and Vidal M. (2009). New best estimates for radionuclide solid–liquid distribution coefficients in soils. Part 3: miscellany of radionuclides (Cd, Co, Ni, Zn, I, Se, Sb, Pu, Am, and others). *Journal of Environmental Radioactivity*, **100**(9), 704–715.

Gimmi T., Leupin O. X., Eikenberg J., Glaus M. A., Van Loon L. R., Waber H. N., Wersin P., Wang H. A., Grolimund D., Borca C. N. and Dewonck S. (2014). Anisotropic diffusion at the field scale in a 4-year multi-tracer diffusion and retention experiment–I: insights from the experimental data. *Geochimica et Cosmochimica Acta*, **125**, 373–393.

Grambow B. (2008). Mobile fission and activation products in nuclear waste disposal. *Journal of Contaminant Hydrology*, **102**(3–4), 180–186.

Gray T., Mann N. and Whitby M. (2007). Periodic Table of Isotopes. Accessed 10th March 2015 through http://periodictable.com/Isotopes/051.123/index.p.full.html

Gruebel K. A., Davis J. A. and Leckie J. O. (1988). The feasibility of using sequential extraction techniques for arsenic and selenium in soils and sediments. *Soil Science Society of America Journal*, **52**(2), 390–397.

Guidebook A. (1989). Measurement of Radionuclides in Food and the Environment. International Atomic Energy Agency, Vienna. Retrieved from https://www.IAEA.org/publications/1398/measurement-of-radionuclides-in-food-and-the-environment Accessed 9th September 2020.

Gustafsson J. P. and Johnsson L. (1994). The association between selenium and humic substances in forested ecosystems—laboratory evidence. *Applied Organometallic Chemistry*, **8**(2), 141–147.

Hampel A., Hansen F. D., Salzer K., Minkley W., Lux K. H., Herchen K., Pudewills A., Yildirim S., Staudtmeister K., Rokahr R. and Zapf D. (2013). Benchmark Calculations of the Thermo-Mechanical Behavior of Rock Salt—Results from a US-German Joint Project. 47th US Rock Mechanics/Geomechanics Symposium, American Rock Mechanics Association, San Francisco, California.

Heberling F., Vinograd V. L., Polly R., Gale J. D., Heck S., Rothe J., Bosbach D., Geckeis H. and Winkler B. (2014). A thermodynamic adsorption/entrapment model for selenium (IV) coprecipitation with calcite. *Geochimica et Cosmochimica Acta*, **134**, 16–38.

Henner P. (2008). Bioaccumulation of Radionuclides and Induced Biological Effects in Situations of Chronic Exposure of Ecosystems a Uranium Case Study. Loads and Fate of Fertilizer Derived Uranium. Backhuys Publishers Leiden, The Netherlands.

Hesslein R. H. (1987). Whole-lake metal radiotracer movement in fertilized lake basins. *Canadian Journal of Fisheries and Aquatic Sciences*, **44**(S1), s74–s82.

Hosseini A., Thørring H., Brown J. E., Saxén R. and Ilus E. (2008). Transfer of radionuclides in aquatic ecosystems–default concentration ratios for aquatic biota in the Erica Tool. *Journal of Environmental Radioactivity*, **99**(9), 1408–1429.

Hoving A. L. (2018). Redox Properties of Boom Clay and their Effect on Reactions with Selenium and Uranium. Doctoral dissertation, UU Dept. of Earth Sciences.

International Atomic Energy Agency (2004). Sediment Distribution Coefficients and Concentration Factors for Biota in the Marine Environment, Technical Reports Series No. 422, IAEA, Vienna.

International Atomic Energy Agency (2010). Handbook of Parameter Values for the Prediction of Radionuclide Transfer in Terrestrial and Freshwater Environments, Technical Reports Series No. 472, IAEA, Vienna.

International Atomic Energy Agency (2014). Handbook of Parameter Values for the Prediction of Radionuclide Transfer to Wildlife, Technical Reports Series No. 479, IAEA, Vienna.

Iida Y., Yamaguchi T., Tanaka T., Kitamura A. and Nakayama S. (2009). Determination of the solubility limiting solid of selenium in the presence of iron under anoxic conditions. Proc. Mobile Fission and Activation Products in Nuclear Waste Disposal, La Baule, pp. 135–145.

Ikonen J. (2017). Sorption and Matrix Diffusion in Crystalline Rocks–In-situ and Laboratory Approach. Doctoral thesis, University of Helsinki, Finland.

Ikonen J., Voutilainen M., Söderlund M., Jokelainen L., Siitari-Kauppi M. and Martin A. (2016). Sorption and diffusion of selenium oxyanions in granitic rock. *Journal of Contaminant Hydrology*, **192**, 203–211.

Irons R., Carlson B. A., Hatfield D. L. and Davis C. D. (2006). Both selenoproteins and low molecular weight selenocompounds reduce colon cancer risk in mice with genetically impaired selenoprotein expression. *The Journal of Nutrition*, **136**(5), 1311–1317.

Jeffery E. H., Wallig M. A. and Tumbleson M. E. (2002). Nutritional toxicologic pathology. In: Handbook of Toxicologic Pathology, 2nd edn, W. M. Haschek, C. G. Rousseaux and M. A. Wallig (eds.), Academic Press, Amsterdam, Boston, Heidelberg, London, New York, Oxford, Paris, San Diego, San Francisco, Singapore, Sydney, Tokyo, pp. 595–629.

Johnson L. H. and McGinnes D. F. (2002). Partitioning of radionuclides in Swiss power reactor fuels (No. NTB--02-07). National Cooperative for the Disposal of Radioactive Waste (NAGRA).

Johnson L. H., LeNeveu D. M., King F., Shoesmith D. W., Kolar M., Oscarson D. W., Sunder S., Onofrei C. and Crosthwaite J. L. (1996). The disposal of Canada's nuclear fuel waste: a study of postclosure safety of in-room emplacement of used CANDU fuel in copper containers in permeable plutonic rock. Volume 2: Vault model (No. AECL--11494-2). Atomic Energy of Canada Ltd.

Joint F. A. O. (2016). Supporting Sampling and Sample Preparation Tools for Isotope and Nuclear Analysis (No. IAEA-TECDOC--1783). Joint FAO/IAEA Division of Nuclear Techniques in Food and Agriculture.

Jones G. D., Droz B., Greve P., Gottschalk P., Poffet D., McGrath S. P., Seneviratne S. I., Smith P. and Winkel L. H. (2017). Selenium deficiency risk predicted to increase under future climate change. *Proceedings of the National Academy of Sciences*, **114** (11), 2848–2853.

Jörg G., Bühnemann R., Hollas S., Kivel N., Kossert K., Van Winckel S. and Gostomski C. L. V. (2010). Preparation of radiochemically pure 79Se and highly precise determination of its half-life. *Applied Radiation and Isotopes*, **68**(12), 2339–2351.

Kaizer J., Dulanská S., Horváthová B., Ješkovský M. and Povinec P. P. (2018). Development of separation procedures for determination of uranium and thorium in the 82 Se source of the SuperNEMO experiment: first steps. *Journal of Radioanalytical and Nuclear Chemistry*, **318**(3), 2321–2327.

Kienzler B., Schlieker M., Rabung T., Borkel C., Geyer F., Hilpp S. and Walschburger C. (2016). Schachtanlage Asse II, Sorptionsuntersuchungen an Gesteinsproben aus der Bohrung Remlingen 15 Teil 1a: Grundwasseranalysen. Auftrag des Bundesamts für Strahlenforschung (BfS), Vol. KIT-INE 002/2016.

Koch-Steindl H. and Pröhl G. (2001). Considerations on the behaviour of long-lived radionuclides in the soil. *Radiation and Environmental Biophysics*, **40**(2), 93–104.

Kowe R., Mobbs S., Proehl G., Bergstrom U., Olyslaegers G., Zeevaert T. and Simon I. (2005). Application of biosphere models in the BIOMOSA project: a comparative assessment of five European radioactive waste disposal sites. *Radioprotection*, **40**(1), S701.

Krivan V. (1982). Role of radiotracers in the development of trace element analysis. *Talanta*, **29**(11), 1041–1050.

Kutschera W. (1998). Dating and environment using long-lived radionuclides. *Il Nuovo Cimento A (1971–1996)*, **111**(8–9), 1019–1031.

Lee C. P., Tsai S. C., Wei Y. Y., Teng S. P. and Hsu C. N. (2008). Comparative study on sorption of individual and coupling cesium and selenium on mudrock. *Journal of Radioanalytical and Nuclear Chemistry*, **275**(1), 115–119.

Lee C. P., Wu M. C., Tsai T. L., Wei H. J., Men L. C. and Hsu C. N. (2012). Comparative study on sorption additivity of individual and coexisting cesium and selenium on bentonite/quartz sand mixtures. *International Journal of Nuclear Energy Science and Engineering*, **2**, 23–27.

Lenz M., Hullebusch E. D. V., Farges F., Nikitenko S., Borca C. N., Grolimund D. and Lens P. N. (2008). Selenium speciation assessed by X-ray absorption spectroscopy of sequentially extracted anaerobic biofilms. *Environmental Science and Technology*, **42** (20), 7587–7593.

Mace N. (2006). Influence de la température sur la rétention du sélénite par une pâte de ciment altérée et par ses phases pures constitutives. Doctoral dissertation.

Magill J., Berthou V., Haas D., Galy J., Schenkel R., Wiese J. W., Heusener G., Tommasi J. and Youinou G. (2003). Impact limits of partitioning and transmutation scenarios on the radiotoxicity of actinides in radioactive waste. *Nuclear Energy-London*, **42**(5), 263–278.

Marguí E., Floor G. H., Hidalgo M., Kregsamer P., Román-Ross G., Streli C. and Queralt I. (2010). Analytical possibilities of total reflection X-ray spectrometry (TXRF) for trace selenium determination in soils. *Analytical Chemistry*, **82**(18), 7744–7751.

Martinčič R. (ed.). (1999). Generic Procedures for Monitoring in a Nuclear or Radiological Emergency. IAEA, Vienna.

Measures C. I. and Burton J. D. (1978). Behaviour and speciation of dissolved selenium in estuarine waters. *Nature*, **273**(5660), 293–295.

Mihailescu A. and Cata-Danil G. H. (2010). Gamma-ray production in the 58 Ni (16 O, X) nuclear reaction. *Romanian Journal of Physics*, **55**(7–8), 712–723.

Natasha T., Shahid M., Niazi N. K., Khalid S., Murtaza B., Bibi I. and Rashid M. I. (2018). A critical review of selenium biogeochemical behavior in soil-plant system with an inference to human health. *Environmental Pollution*, **234**, 915–934.

Neeb K. H. (1997). The Radiochemistry of Nuclear Power Plants with Light Water Reactors. Walter de Gruyter, Berlin and New York.

Nie Z., Finck N., Heberling F., Pruessmann T., Liu C. and Lützenkirchen J. (2017). Adsorption of selenium and strontium on goethite: EXAFS study and surface complexation modeling of the ternary systems. *Environmental Science and Technology*, **51**(7), 3751–3758.

Nothstein A. K., Eiche E., Riemann M., Nick P., Maier P., Tenspolde A. and Neumann T. (2019). Coupling Langmuir with Michaelis-Menten—A practical alternative to estimate Se content in rice?. *PloS One*, **14**(4), e0214219.

Ogra Y., Shimizu M., Takahashi K. and Anan Y. (2018). Biotransformation of organic selenium compounds in budding yeast, Saccharomyces cerevisiae. *Metallomics*, **10** (9), 1257–1263.

Ohlendorf H. M., Santolo G. M., Byron E. R. and Eisert M. A. (2020). Kesterson reservoir: 30 years of selenium risk assessment and management. *Integrated Environmental Assessment and Management*, **16**(2), 257–268.

Olszewska W., Miśkiewicz A., Zakrzewska-Kołtuniewicz G., Lankof L. and Pająk L. (2015). Multibarrier system preventing migration of radionuclides from radioactive waste repository. *Nukleonika*, **60**(3), 557–563.

Ondraf/Niras (NIROND) (2001). Technical Overview of the SAFIR 2 Report, Safety Assessment and Feasibility Interim Report 2. Belgian Agency for Radioactive Waste and Enriched Fissile Materials.

Palattao M. V. B., Hajas W. C. and Goodwin B. W. (1997). Evaluation of the use of ICRP 60 dose conversion factors in a postclosure assessment of a deep geological disposal system (No. AECL--11734). Atomic Energy of Canada Limited.

Parkhurst D. L. and Appelo C. (2013). Description of input and examples for PHREEQC version 3—a computer program for speciation, batch-reaction, one-dimensional transport, and inverse geochemical calculations. *US Geological Survey Techniques and Methods*, **6**, 497.

Pilon-Smits E. A., Winkel L. H. and Lin Z. Q. (eds.). (2017). Selenium in Plants: Molecular, Physiological, Ecological and Evolutionary Aspects. Springer, Cham, Switzerland, Vol. **11**.

Polly R., Heberling F., Schimmelpfennig B. and Geckeis H. (2017). Quantum chemical investigation of the selenite incorporation into the calcite (1014) surface. *The Journal of Physical Chemistry C*, **121**(37), 20217–20228.

Post-closure safety of a deep repository for spent nuclear fuel, Technical Report TR-99-06, Swedish Nuclear Fuel and Waste Management Co. (1999).

Rabung T., Kienzler B., Skerencak-Frech A., Schlieker M., Fellhauer D., Plaschke M., Geyer F., Walschburger C., Kisely T., Böttle M., Fuss M., Altmaier M., Metz V. and Geckeis H. (2018). Schachtanlage Asse II, Sorptionsuntersuchungen an den Gesteinsproben aus der Bohrung Remlingen 15 (Teil 3a). Auftrag des Bundesamts für Strahlenforschung (BfS).

Reamer D. C., Veillon C. and Tokousbalides P. T. (1981). Radiotracer techniques for evaluation of selenium hydride generation systems. *Analytical Chemistry*, **53**(2), 245–248.

Reinfelder J. R. and Fisher N. S. (1994). Retention of elements absorbed by juvenile fish (Menidia menidia, Menidia beryllina) from zooplankton prey. *Limnology and Oceanography*, **39**(8), 1783–1789.

Riaz A., Abbas M. A., Mubeen H., Ibrahim N. and Raza S. (2018). Methods to Enhance Selenium in Wheat through Biofortification: a review. *Journal of Biotechnology and Biomaterials*, **8**(2), 1000282.

Salminen R., Batista M. J., Bidovec M., Demetriades A., De Vivo B., De Vos W., Duris M., Gilucis A., Gregorauskiene V., Halamic J., Heitzmann P., Lima A., Jordan G., Klaver G., Klein P., Lis J., Locutura J., Marsina K., Mazreku A., O'Connor P.J., Olsson S. A., Ottesen R.T., Petersell V., Plant J.A., Reeder S., Salpeteur I., Sandström H., Siewers U., Steenfelt A. and Tarvainen T. (2005). Geochemical Atlas of Europe. Part 1 – Background Information, Methodology and Maps.

Santschi P. H., Li Y. H. and Carson S. R. (1980). The fate of trace metals in Narragansett Bay, Rhode Island: Radiotracer experiments in microcosms. *Estuarine and Coastal Marine Science*, **10**(6), 635–654.

Schilling K., Johnson T. M., Dhillon K. S. and Mason P. R. (2015). Fate of selenium in soils at a seleniferous site recorded by high precision Se isotope measurements. *Environmental Science and Technology*, **49**(16), 9690–9698.

Schilling K., Basu A., Wanner C., Sanford R. A., Pallud C., Johnson T. M. and Mason P. R. (2020). Mass-dependent selenium isotopic fractionation during microbial reduction of

seleno-oxyanions by phylogenetically diverse bacteria. *Geochimica et Cosmochimica Acta*, **276**, 274–288.

Segura R., Pizarro J., Díaz K., Placencio A., Godoy F., Pino E. and Recio F. (2015). Development of electrochemical sensors for the determination of selenium using gold nanoparticles modified electrodes. *Sensors and Actuators B: Chemical*, **220**, 263–269.

Seyler P. and Martin J. M. (1991). Arsenic and selenium in a pristine river-estuarine system: the Krka (Yugoslavia). *Marine Chemistry*, **34**(1–2), 137–151.

Shiobara Y., Ogra Y. and Suzuki K. T. (2000). Exchange of endogenous selenium for dietary selenium as 82Se-enriched selenite in brain, liver, kidneys and testes. *Life Sciences*, **67** (25), 3041–3049.

Spiller H. A. (2018). Rethinking mercury: the role of selenium in the pathophysiology of mercury toxicity. *Clinical Toxicology*, **56**(5), 313–326.

Suzuki K. T., Doi C. and Suzuki N. (2006). Metabolism of 76Se-methylselenocysteine compared with that of 77Se-selenomethionine and 82Se-selenite. *Toxicology and Applied Pharmacology*, **217**(2), 185–195.

Suzuki K. N., Machado E. C., Machado W., Bellido A. V. B., Bellido L. F., Osso J. A. and Lopes R. T. (2014). Removal efficiency of ^{75}Se, ^{51}Cr and ^{60}Co from tidal water by mangrove sediments from Sepetiba Bay (SE Brazil). *Journal of Radioanalytical and Nuclear Chemistry*, **299**(1), 357–361.

StrlSchV (2018). Verordnung zum Schutz vor der schädlichen Wirkung ionisierender Strahlung. Accessed 1st October 2020 through https://www.gesetze-im-internet.de/strlschv_2018/

Tan Z., Wu W., Yin N., Jia M., Chen X., Bai Y., Wu H., Zhang Z. and Li P. (2020). Determination of selenium in food and environmental samples using a gold nanocages/fluorinated graphene nanocomposite modified electrode. *Journal of Food Composition and Analysis*, **94**, 103628.

Tanaka K., Shimada A., Hoshi A., Yasuda M., Ozawa M. and Kameo Y. (2014). Radiochemical analysis of rubble and trees collected from Fukushima Daiichi Nuclear Power Station. *Journal of Nuclear Science and Technology*, **51**(7–8), 1032–1043.

Takata H., Aono T., Tagami K. and Uchida S. (2016). A new approach to evaluate factors controlling elemental sediment–seawater distribution coefficients (Kd) in coastal regions, Japan. *Science of the Total Environment*, **543**, 315–325.

Torres J., Pintos V., Gonzatto L., Domínguez S., Kremer C. and Kremer E. (2011). Selenium chemical speciation in natural waters: Protonation and complexation behavior of selenite and selenate in the presence of environmentally relevant cations. *Chemical Geology*, **288**(1–2), 32–38.

Tuğrul B., Erentürk S., Haciyakupoğlu S., Karatepe N., Altinsoy N., Baydoğan N., Baytaş F., Büyük B., Demir E. and Gedik S. (2015). Kinetic and thermodynamic behavior of selenium on modified bentonite and activated carbon using radiotracer technique. *Acta Physica Polonica A*, **128**(2), 180–181.

van den Berg C. M. G., Khan S. H., Daly P. J., Riley J. P. and Turner D. R. (1991). An electrochemical study of Ni, Sb, Se, Sn, U and V in the estuary of the Tamar. *Estuarine, Coastal and Shelf Science*, **33**(3), 309–322.

van der Sloot H. A., Hoede D., Wijkstra J., Duinker J. C. and Nolting R. F. (1985). Anionic species of V, As, Se, Mo, Sb, Te and W in the Scheldt and Rhine estuaries and the Southern Bight (North Sea). *Estuarine, Coastal and Shelf Science*, **21**(5), 633–651.

Vives i Batlle J., Aoyama M., Bradshaw C., Brown J., Buesseler K. O., Casacuberta N., Christl M., Duffa C., Impens N. R. E. N., Iosjpe M. and Masqué P. (2018). Marine radioecology after the Fukushima Dai-ichi nuclear accident: are we better positioned to understand the impact of radionuclides in marine ecosystems? *Science of the Total Environment*, **618**, 80–92.

Wang Z., Gao Y. X. and Belzile N. (2001). Microwave digestion of environmental and natural waters for selenium speciation. *Analytical Chemistry*, **73**(19), 4711–4716.

World Health Organization (1982). Nuclear power: management of high-level radioactive waste: report on a Working group, Bruges, 2–6 June 1980. World Health Organization. Regional Office for Europe.

World Health Organization (2011). Selenium in drinking-water: background document for development of WHO guidelines for drinking-water quality (No. WHO/HSE/WSH/10.01/14). World Health Organization.

Xu W., Zhu J. M., Johnson T. M., Wang X., Lin Z. Q., Tan D. and Qin H. (2020). Selenium isotope fractionation during adsorption by Fe, Mn and Al oxides. *Geochimica et Cosmochimica Acta*, **272**, 121–136.

Yang Y., Xie Q., Zhao Z., He L., Chan L., Liu Y., Chen Y., Bai M., Pan T., Qu Y. and Ling L. (2017). Functionalized selenium nanosystem as radiation sensitizer of ^{125}I seeds for precise cancer therapy. *ACS Applied Materials and Interfaces*, **9**(31), 25857–25869.

Yao Q. Z., Zhang J., Qin X. G., Xiong H. and Dong L. X. (2006). The behavior of selenium and arsenic in the Zhujiang (Pearl River) estuary, South China Sea. *Estuarine, Coastal and Shelf Science*, **67**(1–2), 170–180.

Yao Q. Z., Zhang J., Wu Y. and Xiong H. (2007). Hydrochemical processes controlling arsenic and selenium in the Changjiang River (Yangtze River) system. *Science of the Total Environment*, **377**(1), 93–104.

Yoneda S. and Suzuki K. T. (1997). Detoxification of mercury by selenium by binding of equimolar Hg–Se complex to a specific plasma protein. *Toxicology and Applied Pharmacology*, **143**(2), 274–280.

Yu L. and Weetjens E. (2016). Application of solubility and transport limited radionuclide release in performance assessment of a spent fuel repository in Boom Clay.